Final Report

Covering the Period March 1976 to August 1979

Prepared Under Contract No. NAS2-9181

September 1979

ROCKET STUDIES OF SOLAR CORONA AND TRANSITION REGION

By

L. W. Acton
E. C. Bruner, Jr.
W. A. Brown
R. A. Nobles

Lockheed Palo Alto Research Laboratory
3251 Hanover Street
Palo Alto, California 94304

For

Goddard Space Flight Center
National Aeronautics and Space Administration

Introduction

The XSST (X-Ray Spectrometer/Spectrograph Telescope) rocket payload launched by a Nike Boosted Black Brant at 16:30:17.934UT on July 3, 1979 was designed to provide high spectral resolution coronal soft X-ray line information on a spectrographic plate, as well as time resolved photo-electric records of pre-selected lines and spectral regions. This spectral data is obtained from a 1 x 10 arc second solar region defined by the paraboloidal telescope of the XSST. The TRC (Transition Region Camera) provided full disc images in selected spectral intervals originating in lower temperature zones than the emitting regions accessible to the XSST. A H-alpha camera system allowed referencing the measurements to the chromospheric temperatures and altitudes.

The payload instrumentation is described more fully in the appended papers by E.C. Bruner, et.al. and W.A. Brown, et.al., references 1 and 2 respectively.

The contract for which this is the final report spanned the time period from March 1976 to August 1979 during which the payload was brought through the detailed design phase, fabrication, optical alignment and first flight. Only a preliminary survey of the engineering and scientific data is reported, since further work on these items is in progress and will be continued under a new contract.

Experiment and Preparations

The rocket payload had completed all prelaunch tests and preparation procedures at the WSMR (White Sands Missile Range), thru the "Vertical" and was ready for launch as of September 27, 1978. At that point a combination of vacuum and command link failures caused a postponement of the mission. The payload was returned to Palo Alto for fault corrections, improvements and

installation of fail safe hardware. On return to Palo Alto the instrumentation was completely disassembled and inspected. The XSST paraboloidal telescope mirror was sent to Imperial College, England where Dr. R.J. Speer performed reflectivity measurements at X-ray wavelengths. His measurements showed that the mirrors' reflective efficiency was about 50% of theoretical at 8 Angstroms and near nominal at 44 Angstroms. He also performed tests with a novel all grazing incidence interferometer which showed the trueness of the mirror surface to better than 0.7 micron. The mirror was then sent to National Physical Laboratory for inspection by Dr. Albert Franks and the addition of a reflecting surface on the front face. When returned to Palo Alto, this additional reflective surface was used to optically establish the direction of the mirror axis. This was then compared with the axis derived from mechanical metrology and the two determinations were found to agree to better than ten seconds of arc.

The curved rail of the XSST, which serves as the optical bench of the 5 meter X-ray spectrometer was removed and sent to Moore Special Tool Company where its profile was remeasured to sub-micron accuracy. This precision aluminum rail was found to have changed remarkably little in the fifteen months since its manufacture. Measurements of the XSST spar made in our laboratory also showed little variation from previous values.

The Spiraltron electron multipliers in the XSST detector system were checked and found functional, despite the electrical breakdown in the tower at WSMR. Detail measurements of the Spiraltron pulse height distribution in relation to the discriminator settings showed all detectors to have acceptable performance. Other tasks completed prior to payload re-assembly included:

- o Hα optical systems support bracket improvement
- o Hα system alignment checked and re-set
- o Hα Video Camera checked and repaired
- o Shroud heaters repaired

- o Heater controls repaired
- o Rewiring to give independent High Voltage control
- o Calibration of pressure sensors
- o Fabrication of umbilical and break out box
- o Made hole in front bulkhead for XSST alignment mirror
- o Vacuum tests and outgassing
- o Spectroscopic plate processing tests
- o Pre-integration with SPARCS.

The alignment sensor for the paraboloidal X-ray mirror of the XSST was carefully analyzed and brought up to operational status.

After the complete disassembly for these component checks, the XSST was re-built with the aid of precision mechanical metrology using techniques learned during the first assembly exercise in August 1978.

Figures 1 and 2 show views of the XSST mirror mounted on its shipping container base. The photographs were taken before the auxillary reflective surface was added to the mirror front. Figure 3 shows the mirror mount cell with a dummy aluminum mirror installed. Figure 4 shows the XSST optical bench, rail with the slit, grating and camera installed. In Figure 5, the camera back is removed, showing plate holder, spiraltron detectors and associated electronics circuitry. Figures 6 and 7 show right and left side views of the complete payload minus the TRC. If installed, a portion of the TRC would be visible through one of the holes on the left hand side.

Fielding Efforts at WSMR

After completion of modifications, assembly, alignment and testing at Palo Alto and SPARCS pre-integration at Sunnyvale, the payload was shipped

back to WSMR. The WSMR efforts included rechecking alignments, calibrations, SPARCS integration, suntracking, ASCL tests, vacuum tests, horizontal test, vertical air bearing, ASCL flight practice, film loading and vertical test. These efforts went very smoothly and without major problems. The smoothness of the fielding operation was in part due to a good state of prefielding readiness together with excellent support at WSMR by SRD, SPARCS and NMSU/PSL.

The most serious prelaunch problem encountered was a vacuum leak at the trap door after the rocket was loaded in the tower and the payload on the TVRS (Tower Vacuum Retraction System). The fix required unloading the rocket and separating the payload. The problem was caused by a displacement of the trap door's semi-capative O-ring seal and was cured by simply replacing the O-ring in its groove.

Flight and Recovery

The rocket was launched from the LC36 tower facility on July 3, 1979. The maximum elevation reached was 300 km and the time above 120 km was about 383 seconds. The systems for launch, despin, separation, sun-acquisition by SPARCS and control by ASCL all performed perfectly. The recovery point was about 114 km almost due north of the launch site on nearly level ground. The payload was recovered intact, essentially undamaged and with secure film compartments. However, vacuum had been lost, as the front trap O-ring had become displaced in flight and its wiring harness partially burned off and entrapped when the door closed.

Mission Objectives and Performance

Following is a summary list of mission objectives together with an indication of the success achieved. A plus (+) indicates success, zero (0) failure and (P) a partial success.

Mission Objectives

+	Launch, despin, separation and acquisition of sun by SPARCS.
+	Acquisition by SPARCS to pre-programmed location.
+	300 seconds above 120km.
+	Fine pointing to $\pm$ 1 arc sec for TRC exposure.
0	X-ray spectrum on photographic film.
P	X-ray photoelectric data.
+	Telemetry of X-ray photoelectric data.
+	Telemetry of UV data from central image detector of XSST.
+	Scan of active regions using ASCL system.
+	One or more UV images from TRC.
+	Video presentation of solar image by H-alpha telescope.
+	Opening and closing of XSST shutter.
+	Operation of TRC shutter, filter wheel and film drive.
+	Operation of H-alpha framing camera.
+	UV images of solar disc on TRC film.
+	H-alpha images on framing camera film.
+	Operation of alignment measurement system
+	Minimal in-flight deflection of spar.
+	Temperature and pressure records.
+	Recovery of paylaod intact with film compartment secure.

Anomalies Encountered

1. The flight electronics PCM failed on the UV and all 12 photoelectric detector channels. It was apparently OK pre-launch, intermittent prior to T + 75 and failed at that point. As a result of this failure, the primary ASCL peek-seek algorithm was not able to function properly and hence the X-ray exposure did not end up on a bright feature. The problem was in the on-board electronic instrumentation section, which has been returned to SPARCS for analysis and repair. All detector channels worked all right, but since the exposure was not taken on a bright spot the X-ray signal levels were low and it is difficult to evaluate the background level. It is quite certain that X-rays were detected but at the present stage of the analysis it cannot be claimed that a spectrum was recorded.

2. Re-entry into the atmosphere and loss of stable pointing occurred much sooner than anticipated. This early re-entry was partially responsible for a short (approx. 2 seconds) period of corona discharge in the Spiraltron photoelectron detectors.

3. The X-ray plate on the XSST was heavily fogged. The reason for this is not known for certain at present, but there is evidence that an unexpected large mount of scattered UV radiation was present, fogging the plate and making it impossible to see the faint X-ray spectrum which should have been recorded. A second possibility is the short exposure to corona discharge in the adjacent detector assembly when the payload re-entered the atmosphere. An all out effort will be made to eliminate this fogging on the next flight.

4. The H-alpha film camera was not framing properly, although all aspect data are OK. This camera unit has been a continual headache and a strenuous effort will be made to either replace or improve its performance in the future.

5. The H-alpha filter was off-band during the flight resulting in a loss of contrast. Although this is not a critical problem, an effort will be made to replace it or improve its performance on the next flight.

6. The front trap door lost its O-ring in flight and its wiring harness partially burned off and became entrapped when the door closed. The unit has been returned to GSFC for rework of O-ring groove and the screws that hold the hinge. Next flight the door will be closed by command to assure no aerodynamic heating of the payload interior, and to help insure recovery in an evacuated condition.

7. One of the redundant pressure sensors was non-operational during the flight.

8. The payload pressure appeared to drift up during the flight. This is not understood at present. The sensor calibration will be checked to see if the effect is real. It if is, outgassing sources will be sought, such as, for example, the film during the TRC and H-alpha camera operation.

9. Somehow the device that mixes a time indicator with the ASCL TV in the ASCL room at N-200 caused an intermittent distortion of the signal. Presumably PSL will be looking into the problem.

10. The cryogenic pumps on the TVRS loaded up and could not be properly baked out. These should be replaced with pumps which do not load up and which do not require the difficult struggle of handling the large bottles of LN_2 in the tower. The TVRS itself operated very well on this mission.

X-Ray Photoelectric and UV Flight Data

The X-ray spectrometer data is contained in the 12 Spiraltron and UV central image detector (CID) channels. The detectors are set to look at the following lines; Ne X, 12.13Å, Ne IX, 13.45Å, Fe XVII, 15.01Å, O VIII, 18.97Å O VII, 21.60Å, N VII, 28.79Å, C VI, 33.74Å, C V, 40.27Å, and the CID at 1450 to 2000Å. Three additional Spiraltron channels are set to sample the X-ray background level in the 12 to 40Å wavelength interval.

Most of the X-ray data analysis to date has involved the channels corresponding to the Fe XVII, O VII and C VI lines, which are designated as "prime channels". Serial and spatial plots of the counting rates in these channels have been made to evaluate the correlation of their signal intensities with other spatial features seen in H-alpha and with spatial features detected by the CID.

The X-ray counting rates were low throughout the flight except for the first few seconds after turn-on of the Spiraltron high-voltage power supplies. Some higher counting rates seem to show some spatial correlation, and late in the flight, when the rocket pointing was stationary, there is at least one period of enhanced counting in the X-ray lines. More work needs to be done to determine the extent to which these signals are real. CID counting rates were about 300 per second throughout with significant variations during the pointing exercises and clear turn ons and offs during the limb crossings.

The approximate position of the raster scan on an H-alpha image of the solar disc is shown in Figure 8. The photograph shown is courtesy Chas. Welch and was taken with the ground based telescope at N-200. However, the same pointing information is available from the on-board H-alpha telescope camera but with poorer image contrast. Some samples of the data are given. The coarse scan data

plotted serially in Figure 9, shows total counts in each 1.56 second duration scan box. The upper trace is the UV or CID data, the middle trace data the sum of the three prime X-ray channels and the lower trace, which gives an indication of the noise background, is data acquired during the previous days vertical simulation in the three prime channels. Figure 10 is a serial trace for all 12 X-ray channels, during the coarse scan, and Figure 11 shows serial traces for channel 2, Ne X and two background channels, 1 and 12, during the coarse scan. Figure 12 shows a trace of the UV counts in intervals of about 0.7 seconds.

Flight Engineering Data

Some representative in-flight engineering data are presented in the following figures. Figure 13 gives readings of the pitch and yaw XSST alignment position sensors. As can be seen, after the transients during about the first 60 seconds, the alignments remained relatively constant throughout the flight. Temperatures of the forward and aft portions of the spar are shown in Figure 14. Again after initial transients the temperature remained fairly constant until the on-set of aero-dynamic heating near the end. The records indicate a minimal fore to aft temperature gradient. Figure 15 is the H-alpha filter temperature, which started at about 38.6 ^{o}C at T = 0, dropped rapidly during the first 100 seconds and then more slowly through the remainder of the flight. Since the nominal"on band" temperature is 42^{o}C, this record partially explains the poor flight performance of the filter. The evidence strongly suggests that the on-board filter heater was non-functional.

Instrument Mechanical Stability

One of the principle challenges of the XSST program has been the provision and maintenance of the required alignment accuracy in the flight instrumentation. Considerable attention was given this matter in the design phase as well as in assembly and alignment verification procedures. Table 1 gives a brief summary of the results of some pre- and post flight alignment measurements, which evidence the general stability and robustness of the instrument design. In Table 1, measurements the spectrometer mechanical axis was established by mechanical and optical metrology. The direction of the paraboloidal mirror front and the LISS (Lockheed Intermediate Sun Sensor) was established by optical autocollimation and the H-alpha direction by sighting on the cross-hairs through the H-alpha telescope optics. The XSST direction is that given in data by A. Franks and M. Stedman, National Physical Laboratory.

From the table it can be seen that the most significant shift was a pitch direction movement of the LISS from 26 to 78 arc seconds with respect to the instrument mechanical axis. This is probably a result of the heating experienced in the area of the front plate during re-entry.

The roll position stability of the mirror was determined by supporting the spar on guage blocks and measuring the height of each of the four corners of the mirror base above a precision surface table. The pre-flight sequential measurements for the corners were 0, -5.6, -18.6 and -3.7 microns and post-flight 0, 0, -145 and -139 microns respectively. Comparison of these measurements indicates a substantial rotation of the mirror, or alternatively of the spar as a whole, about the horizontal axis. To determine which of these two possibilities pertain, the spar was turned over and supported on gauge blocks with its bottom side up and measurement made of the distance

of the six pads from the surface table. Comparison with similar pre-flight measurements indicated that the only significant change was a 120 micron upward movement of one of the pads. This pad, located just aft of the central bulkhead, is one of the three on which the payload is supported for the mirror height measurements. The movement of this pad is just that needed to account for the apparent mirror rotation noted above. Since the alignment sensor reading indicated no movement during flight it appears that the skin on the spar in the neighborhood of the pad was strained, possibly as a result of a sideward landing impact. This relatively minor movement can easily be accomodated during the build-up for the next XSST flight. The good flight alignment plus the relatively minor strain producted by the heavy land impact stress attests to the overall adequacy of the XSST mechanical design.

Spectrometer Pointing Direction

Knowledge of the pointing direction of the approximately 1 x 10 arc second field of view of the XSST spectrometer system was derived from metrology and geometry considerations. Limb crossing signals from the UV CID channel during the July 3rd flight provided an opportunity of actually checking the pointing with respect to the H-alpha telescope.

Early in the flight, at about t = +87 seconds, the solar disc was seen to come into the field of view of the H-alpha video monitor and sweep across the field, reverse direction and slowly stabilize with three limb crossings taking place in an interval of less than 2 seconds. Figure 16 shows schematically the order in which the H-alpha crosshairs swept across the limb. Since the UV sensor in the XSST CID system was on continuously the UV data show these limb crossings. The high data rate available in the telemetry makes it possible to compare the position of the limb in the H-alpha video monitor presentation, which included a real time indicator, and the cumulative counts in the CID channel. For example, Figure 17 is a plot of the counts in the UV channel as the limb was crossed the third time. From this plot it can be seen that the UV limb came into the field of view of the XSST at t = 89.16 sec (16:31:46.1 UT). Figure 18 is a tracing of the video monitor while playing back the flight tape frame by frame and tracing the position of the H-alpha limb, and noting the time in each frame traced. The two dashed limb traces correspond to the turn-on time of the UV signal as determined from Figure 17. Similar curves were generated for the second and first limb crossings. The first limb crossing was least reliable because the video image in the first crossing was somewhat less well defined presumably due to the rapid change in intensity as the sun came into the field of view for the first time. Figure 19 is an overlay

combining the limb crossing data from the second and third crossings. Also included in this figure are tracings of three identifiable sunspots, which when compared with the full sun H-alpha photograph provided by Welch, gives the scale of the image. These data indicate that the offset of the XSST field of view from the H-alpha crosshair is 144 arc sec in yaw and 100 arc sec in pitch, whereas from metrology and geometry considerations the offset was believed to be no more than about 10 arc seconds in either pitch or yaw. The source of this discrepency is not understood at the present time.

The cause of the misalignment cannot be blamed on the shift of position between the rail and the mirror found in the post flight metrology (discussed above). Because the alignment sensor indicates that the shift occurred after the flight and its magnitude, in any case, appears to be less than that necessary to produce the alignment error discussed here. No flaw has yet been found in the analysis of the UV limb crossing data. The relatively good agreement between the results from the second and third crossing which were in opposite directions together with the rough agreement with those of the first crossing, rule out systematic errors in interpretation such as timing errors, size of XSST field of view errors or large differences between the position of the H-alpha limb and the UV limb. Likewise a review of the metrology notes on the many times repeated measurements of the positions of the mirror, slit, etc. have failed to reveal a problem in these measurements.

However, two crucial items were never checked at Palo Alto, one, the actual position of the slit within the slit block and the other, the position of the focus of the mirror. Our metrology has verified NPL's specification of the orientation of the mirrors' axis of rotation but no measurement was made of the focus position. An attempt will be made to verify the focus position, as an error of 0.7mm would explain the apparent UV and H-alpha alignment

discrepancy. It appears that there must be an error in the slit location or of the focus position or else there is a weak link in the chain of reasoning which gives the XSST pointing direction from the metrology data. Work is continuing on the resolution of the discrepancy.

TRC Results

The results obtained by the LPSP* team headed by Roger Bonnet using the Transition Region Camera were excellent. A joint paper describing the results of full disc photography with the narrow band ultraviolet filters is in preparation in France. The indium filter for the 977Å C III line failed and the two C IV filters set for on and off the 1548Å doublet gave only marginal results due to storage and handling problems associated with these advanced filters, but the Lyman alpha filter gave photographs of unequalled definition. These photos showed for the first time spicules on the limb and on the disc in L-alpha and magnetic complexity in active regions on the limb and on the disc. Features of size less than one arc second were observed, limited only by the resolution of the 101-01 film. The LPSP team is eager to repeat the experiment with a somewhat different filter set making use of the experience gained on the first flight. Figure 20 is an example of a Lyman alpha filtergram.

* Laboratoire de Physique Stellaire et Planetaire
CNRS
Verrieres le Buisson, France

Summary and Conclusions

Our objectives in developing this new solar rocket payload were to extend the state of the art of space borne high resolution spectroscopic instrumentation into the 10 to 50 Angstrom spectral region and to explore the solar corona emission in this spectral region simultaneously with ultraviolet measurements in the chromosphere-corona transition region. While not all objectives were met in the first flight, it has demonstrated the feasibility of building and flying a sophisticated instrument of this type.

The design, construction and alignment of an optical instrument based on high accuracy machining and metrology was a challenging engineering problem. While difficult, the technique has the advantage that the final alignment can be carried out in ambient laboratory conditions, avoiding a tedious series of trial exposures in a vacuum system. Rechecking of alignment was done in the field, again without resort to vacuum. Finally, since the construction and alignment of the instrument is based on accurate mechanical measurements, we expect to be able to measure absolute wavelengths of lines observed in later flights of the high-resolution version of the XSST with high confidence and to derive Doppler velocities.

Engineering and scientific data obtained from the first flight is only partially analyzed and work on this will continue as part of the solar corona rocket program.

Table 1

Pre- and Post Flight Alignment Comparisons

Pitch Direction	Pre-Flight (arc seconds)	Post-Flight (arc seconds)
Mechanical Axis (reference)	0	0
Paraboloid Mirror Front	39	41
LISS	148	149
H-Alpha	148	131
XSST	160[a,b]	185[b]
Yaw Direction		
Mechanical Axis (reference)	0	0
Paraboloid Mirror Front	15	5
LISS	26	78
H-Alpha	40	37
XSST	51[a]	-46[b]

Measurement accuracy varies from about ± 2 to ± 5 arc seconds depending on the measurement complexity.

a) By mechanical metrology and calculation

b) By observation

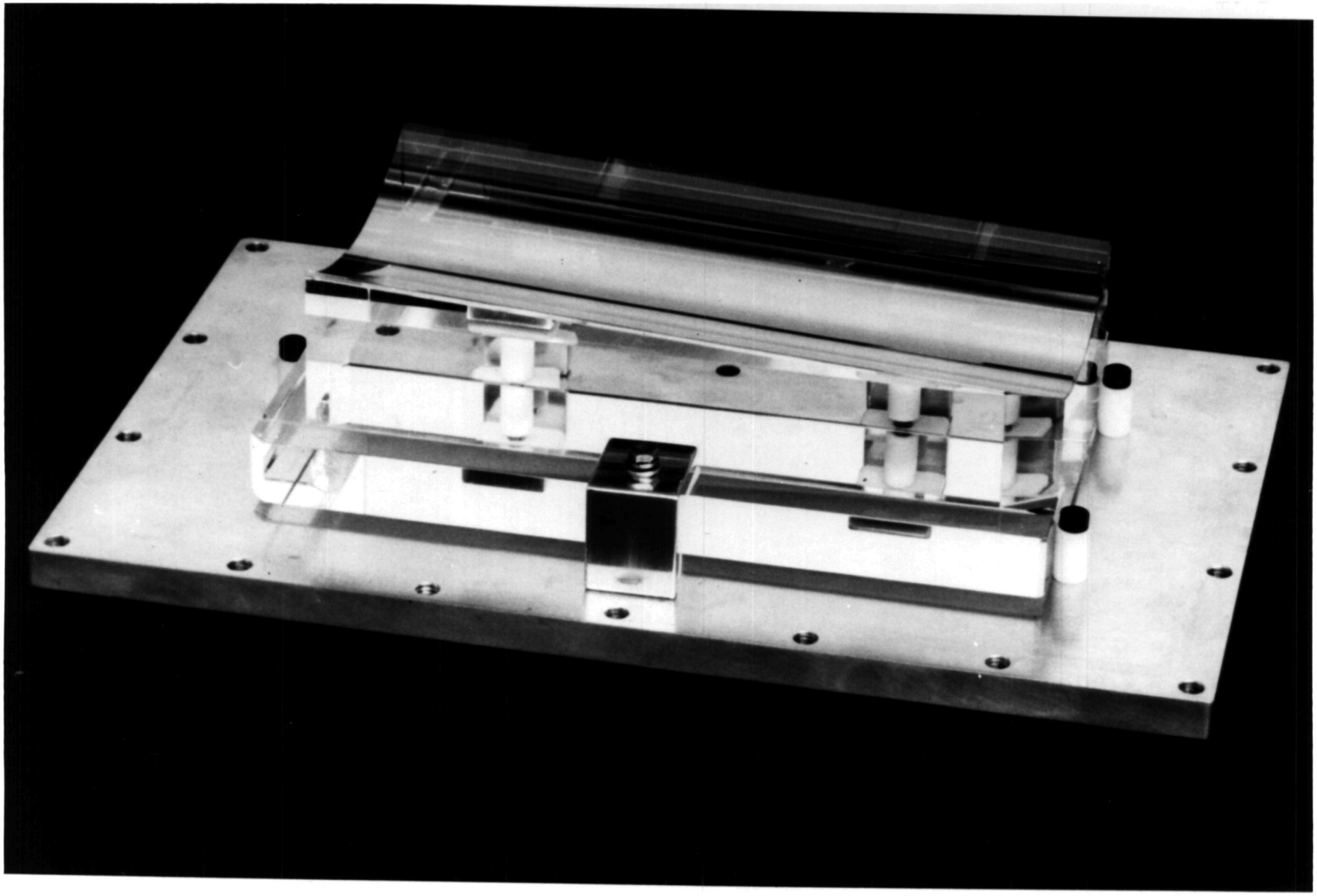

Figure 1. XSST Paraboloidal mirror mounted on base of shipping container.

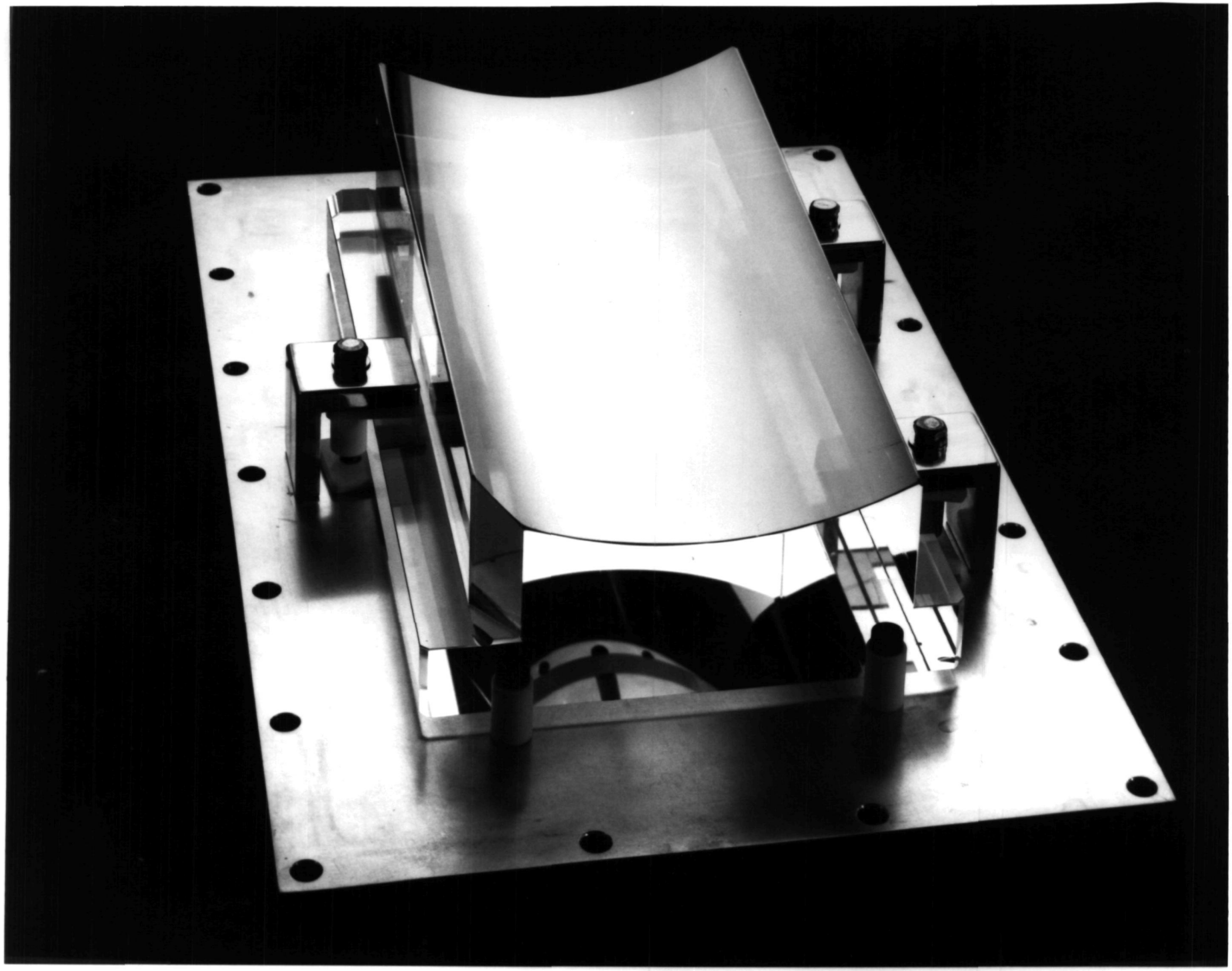

Figure 2. Front view of XSST paraboloidal mirror.

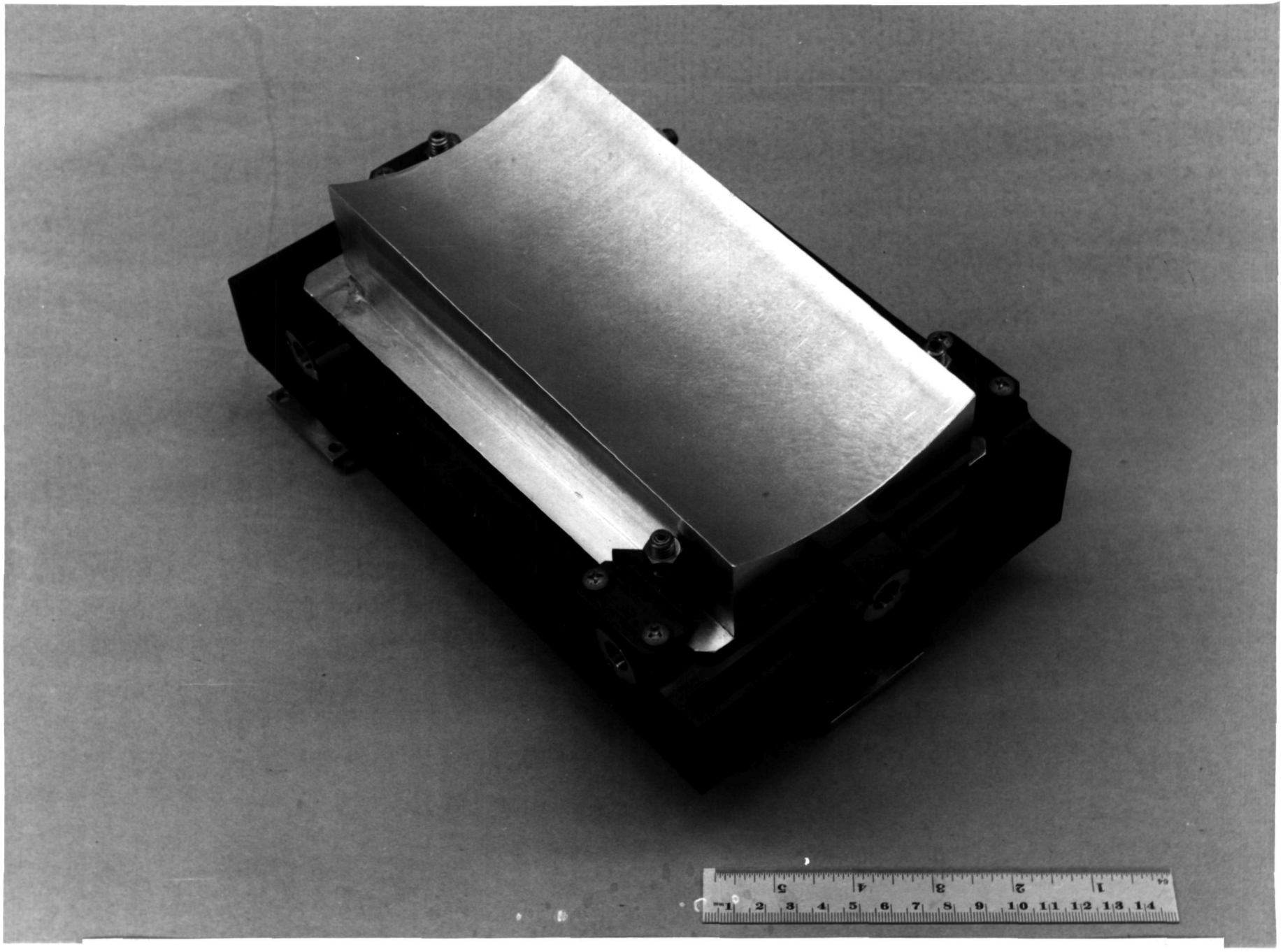

Figure 3. Aluminum mass model of the XSST paraboloidal mirror mounted in the flight mirror holder.

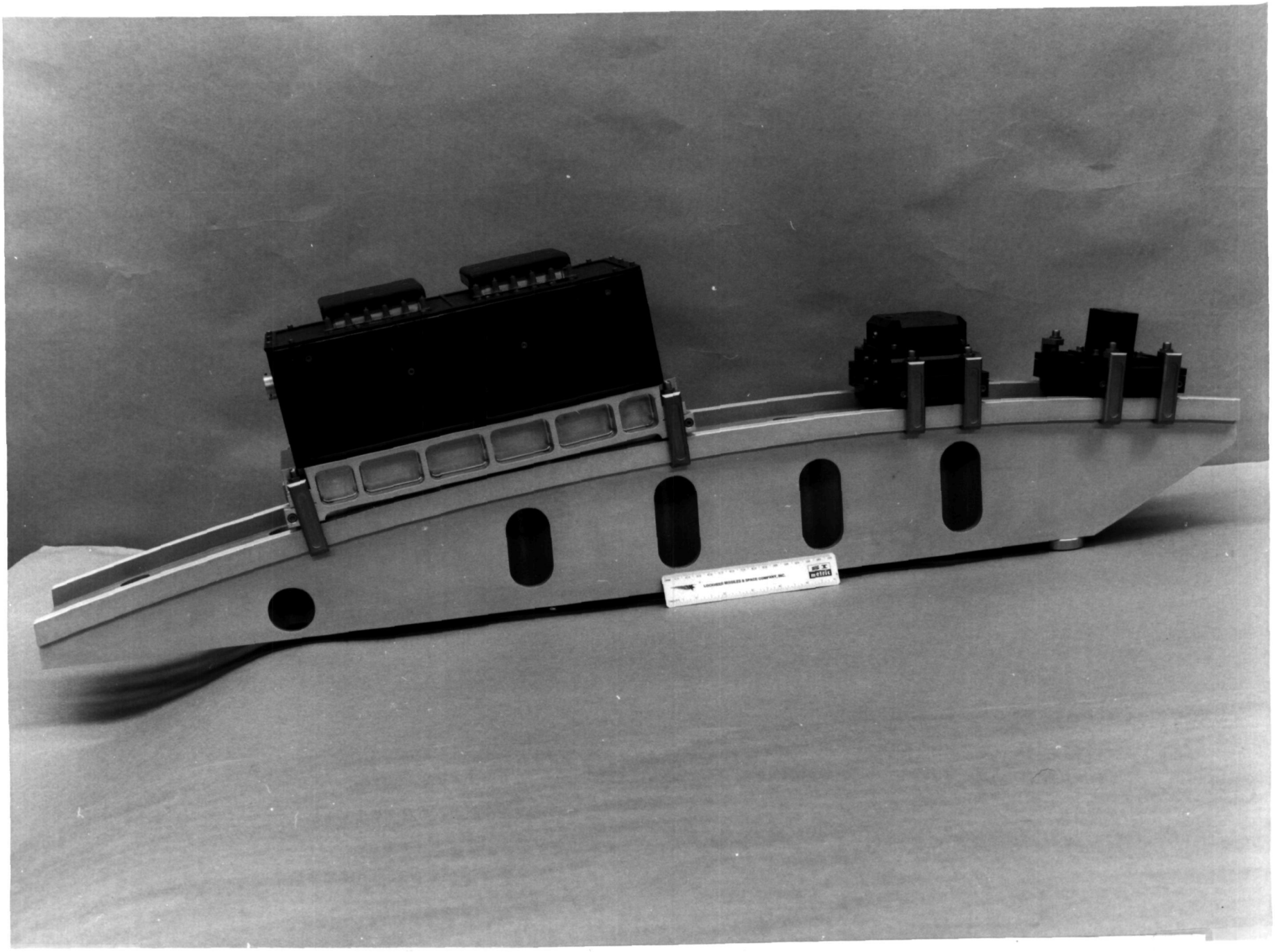

Figure 4. XSST spectrometer assembly showing curved optical rail, detector assembly, grating holder and slit holder. All parts are aluminum except steel clamps which secure them to the rail.

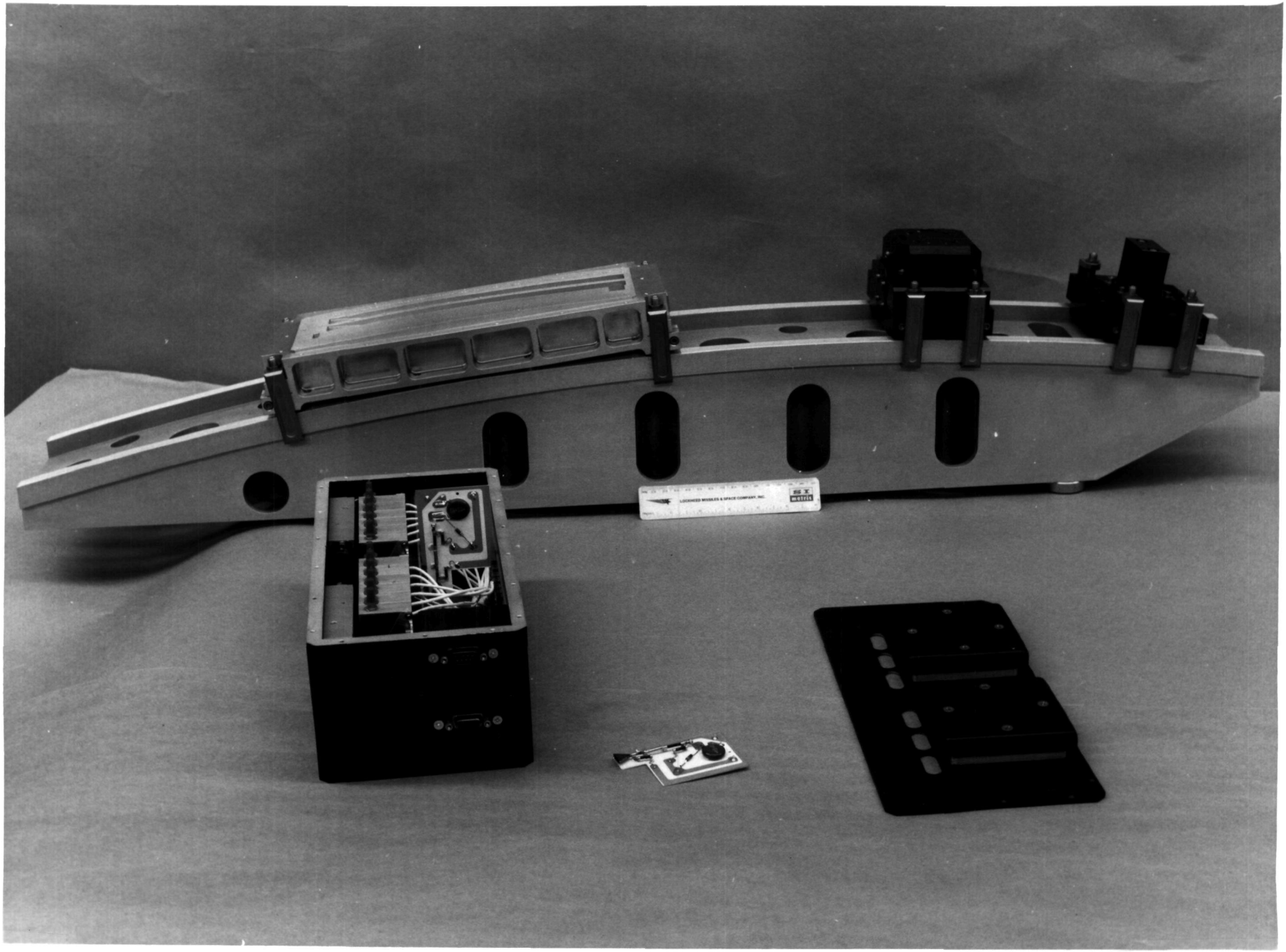

Figure 5. Partial disassembly of XSST detector section showing one of the Spiraltron assemblies partially inserted and one lying next to the box.

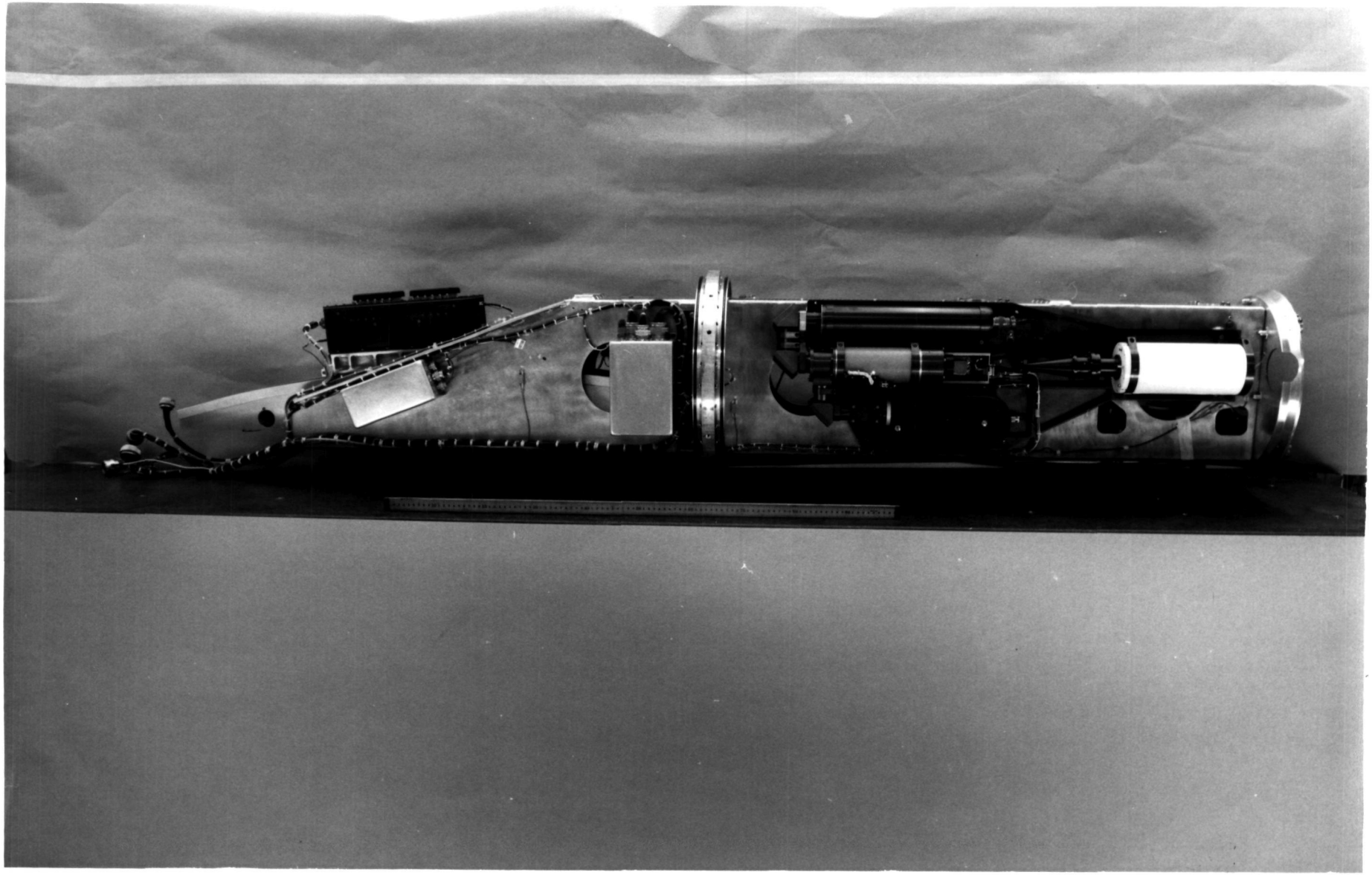

Figure 6. Right hand view, Solar Rocket payload with skins removed. On this side the H-alpha system with video and 35mm cameras is visible.

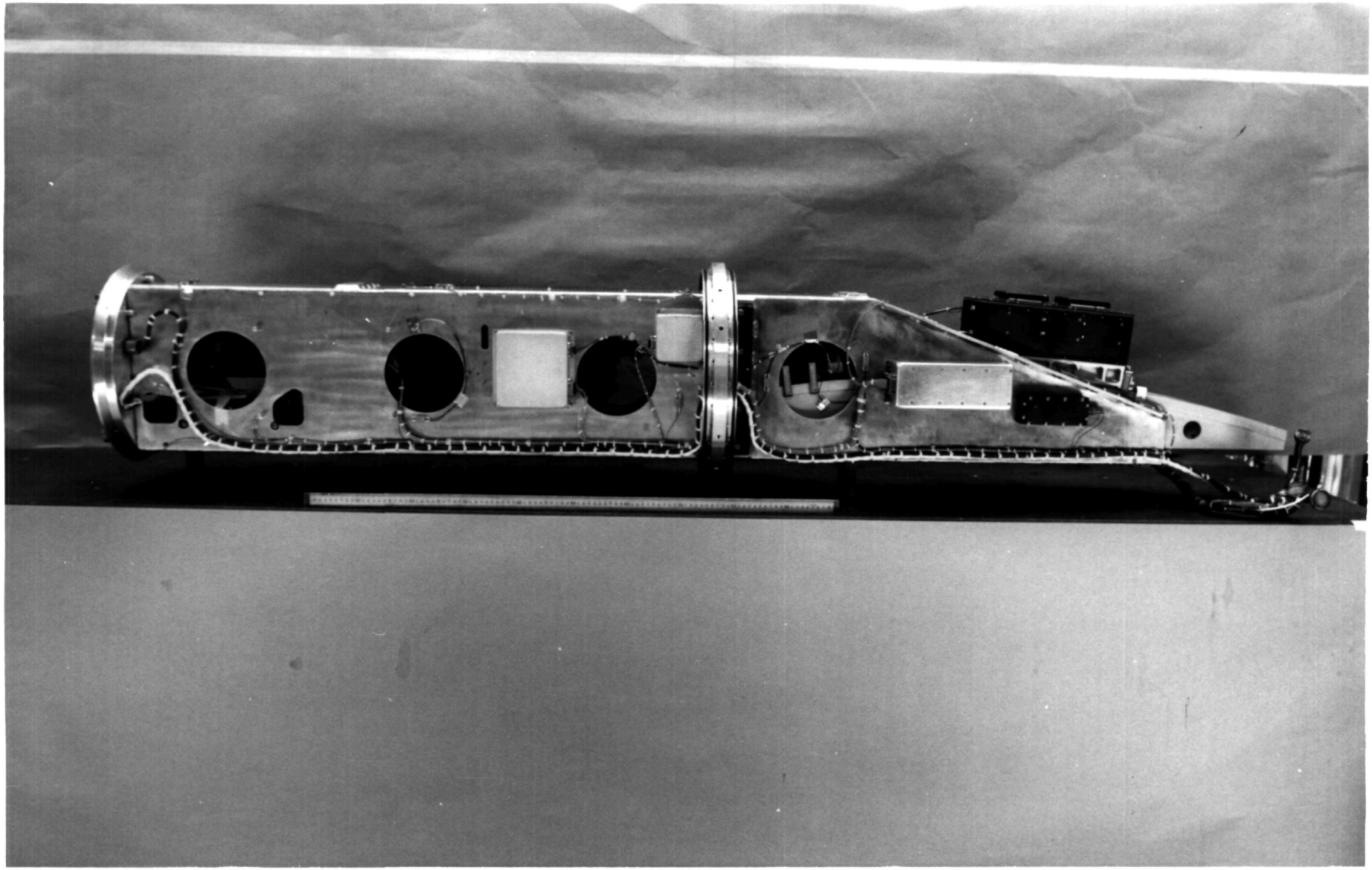

Figure 7. Left hand view of payload. The TRC has been removed for return to LPSP in France.

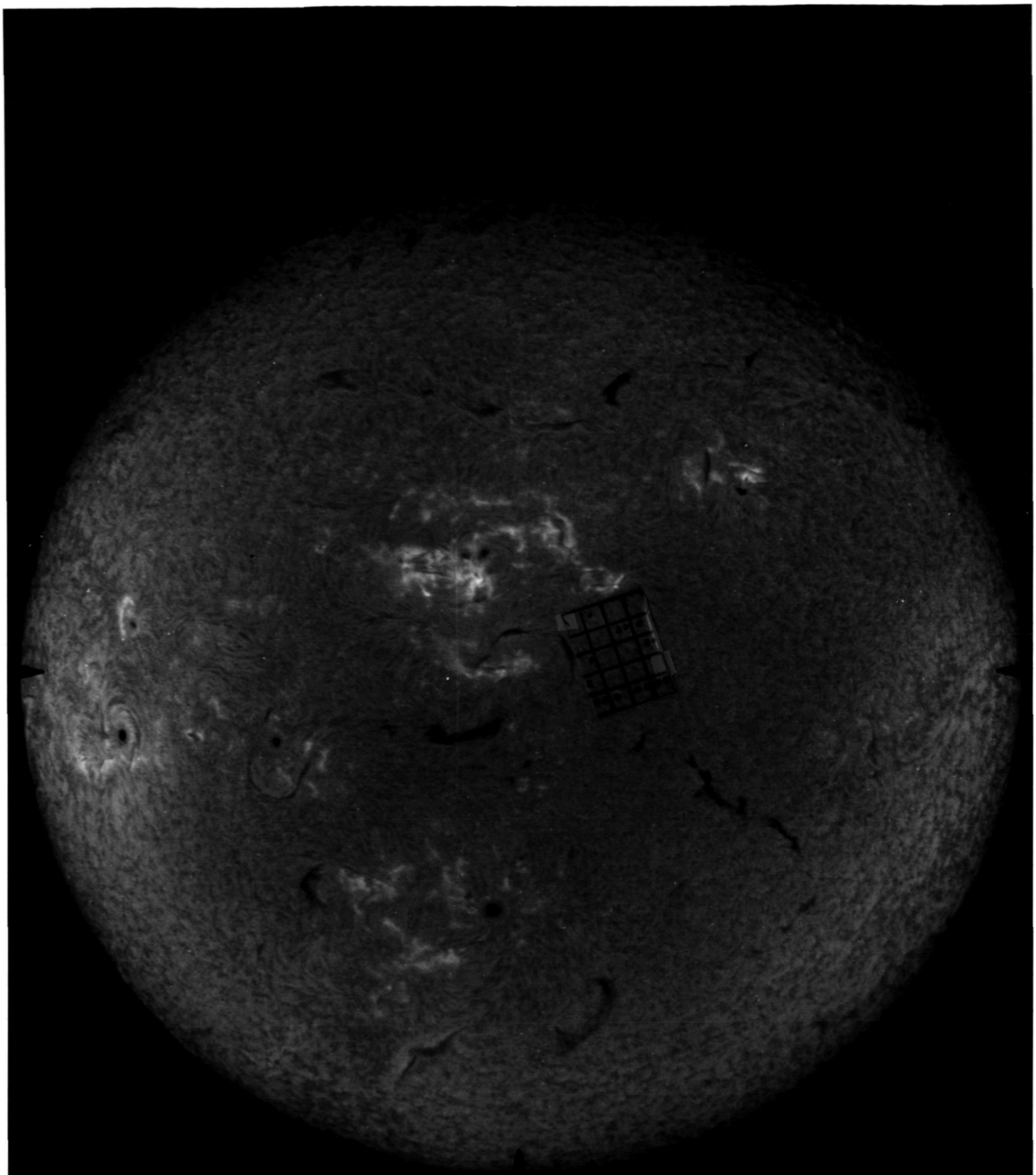

Figure 8. H-alpha photograph (ground based telescope at WSMR, C. Welch) with approximate location of coarse scan. Further analysis may alter this position.

Figure 9. X-ray and UV counting during coarse scan sequence. Upper trace contains UV counts, with legend at right. Lower trace, sum of three prime X-ray channels during vertical test. Middle trace, three prime channels during flight, legend at left. Abcissa marked in scan cell numbers, for 5 rows of 8 steps per row, first and second digits give row and step number respectively. (Duration of each step is about 1.56 sec. This data has not been corrected for a half second delay between ASCL command and pointing motion.) The diamond indicates the cell selected for the fine scan.

Figure 10 Sum of all 12 x-ray channels during the coarse scan. Abcissa identification same as Figure 9.

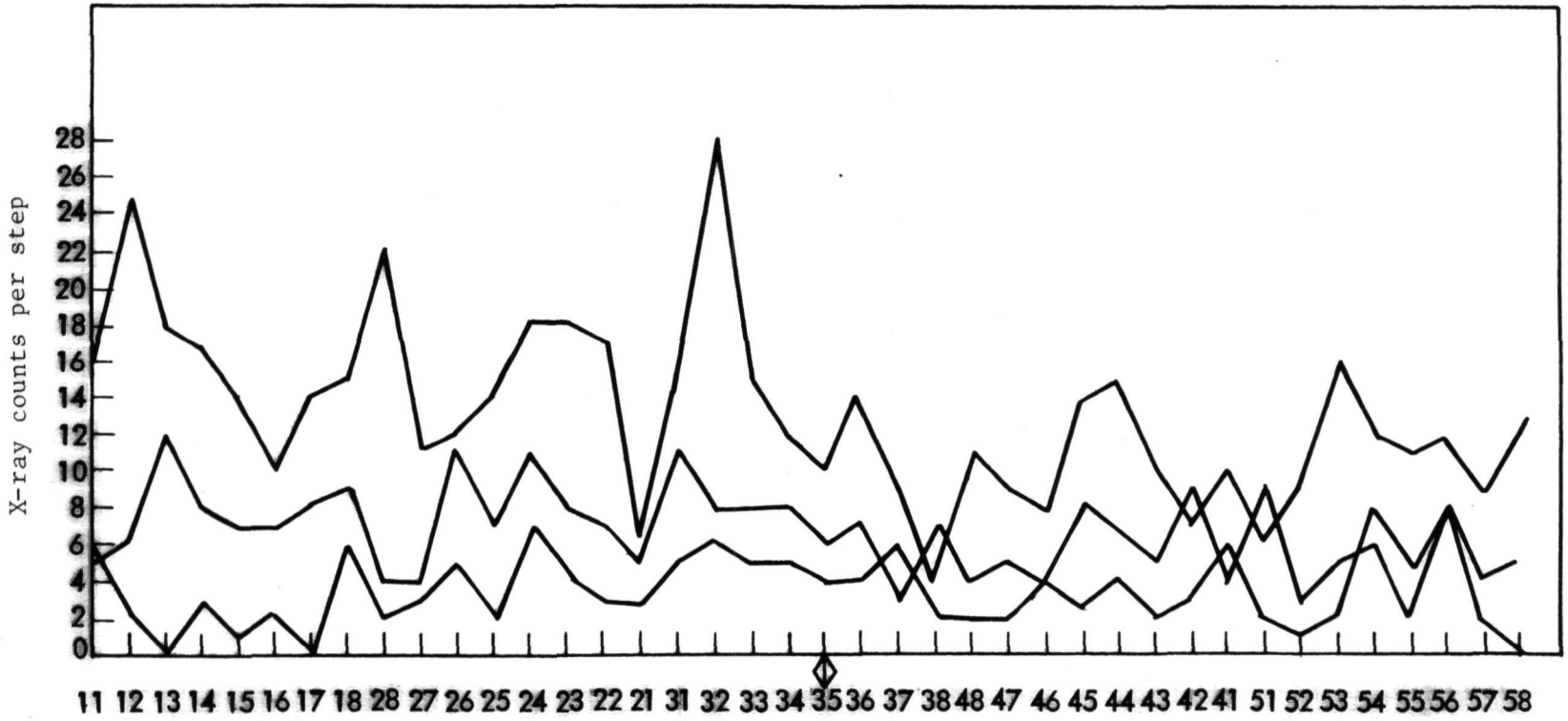

Figure 11 Counts during coarse scan in channels 2,1, and 12 (from top to bottom)
Abcissa identification same as Figure 9.

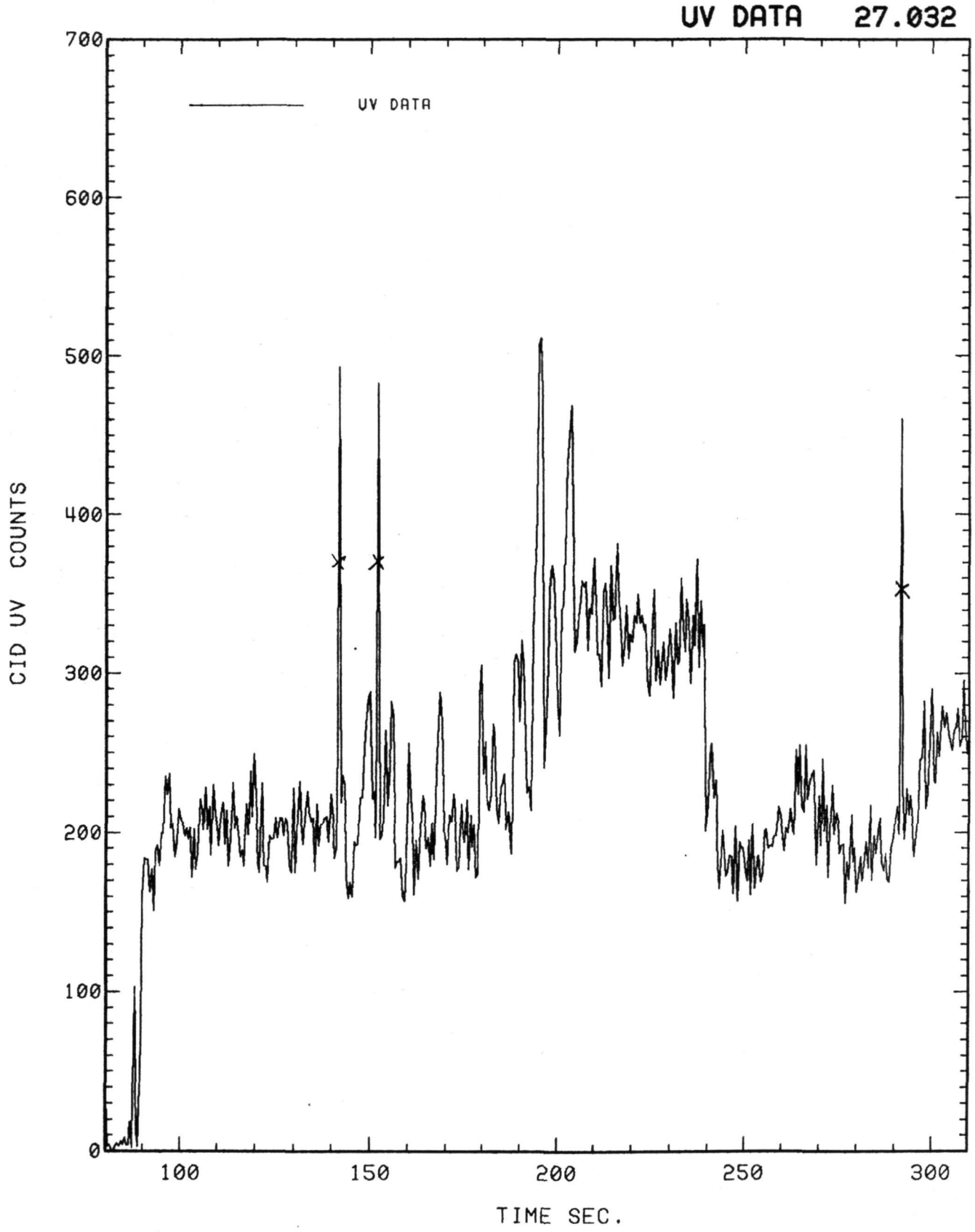

Figure 12. Central Image Detector counts per .7 sec during entire flight. Most of the extreme spikes are not real and further data processing will correct this.

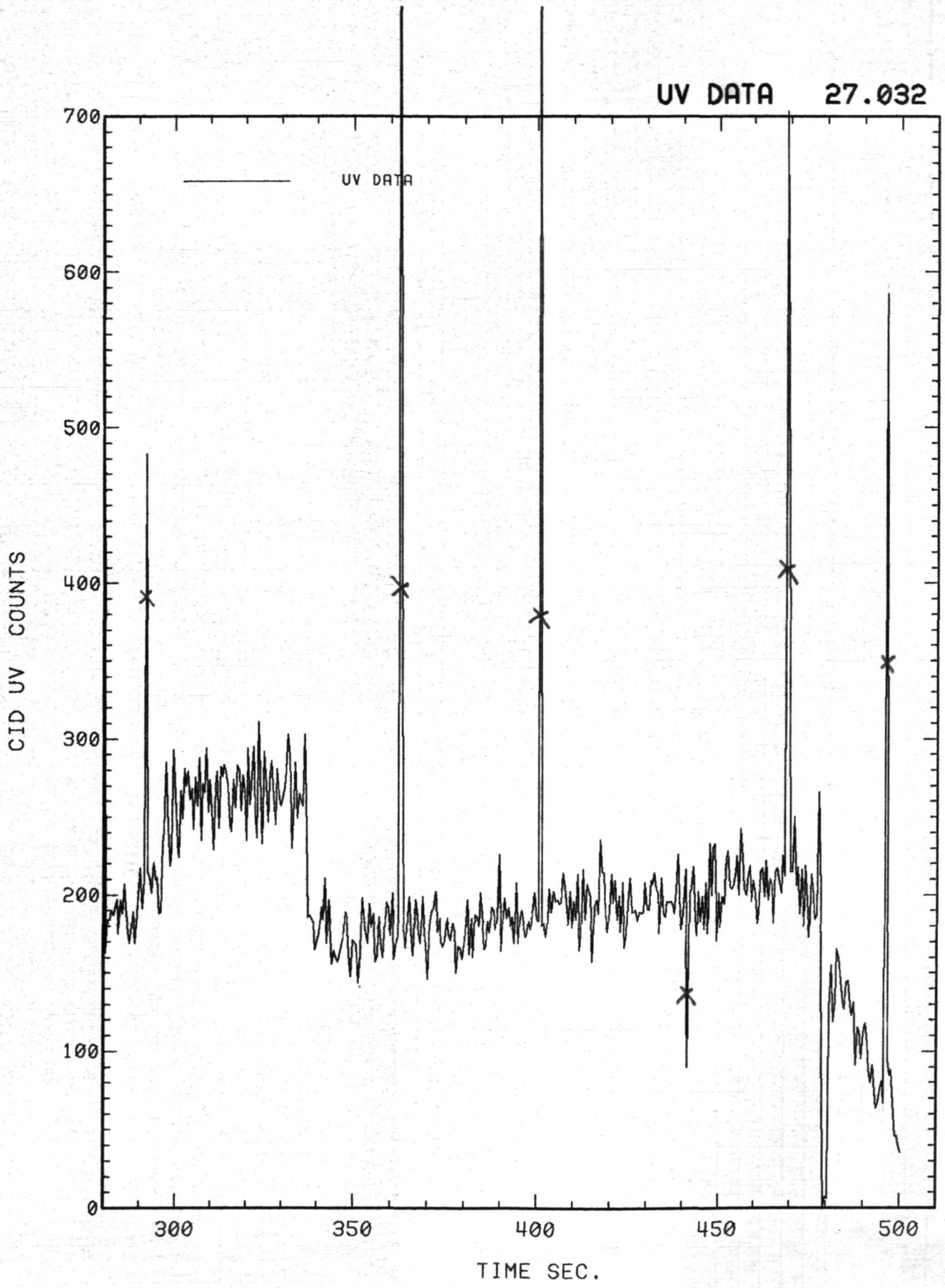

PLOT NO. 1 DONE AT 9:16 ON FRI, 31 AUG., 1979

Figure 12, part 2

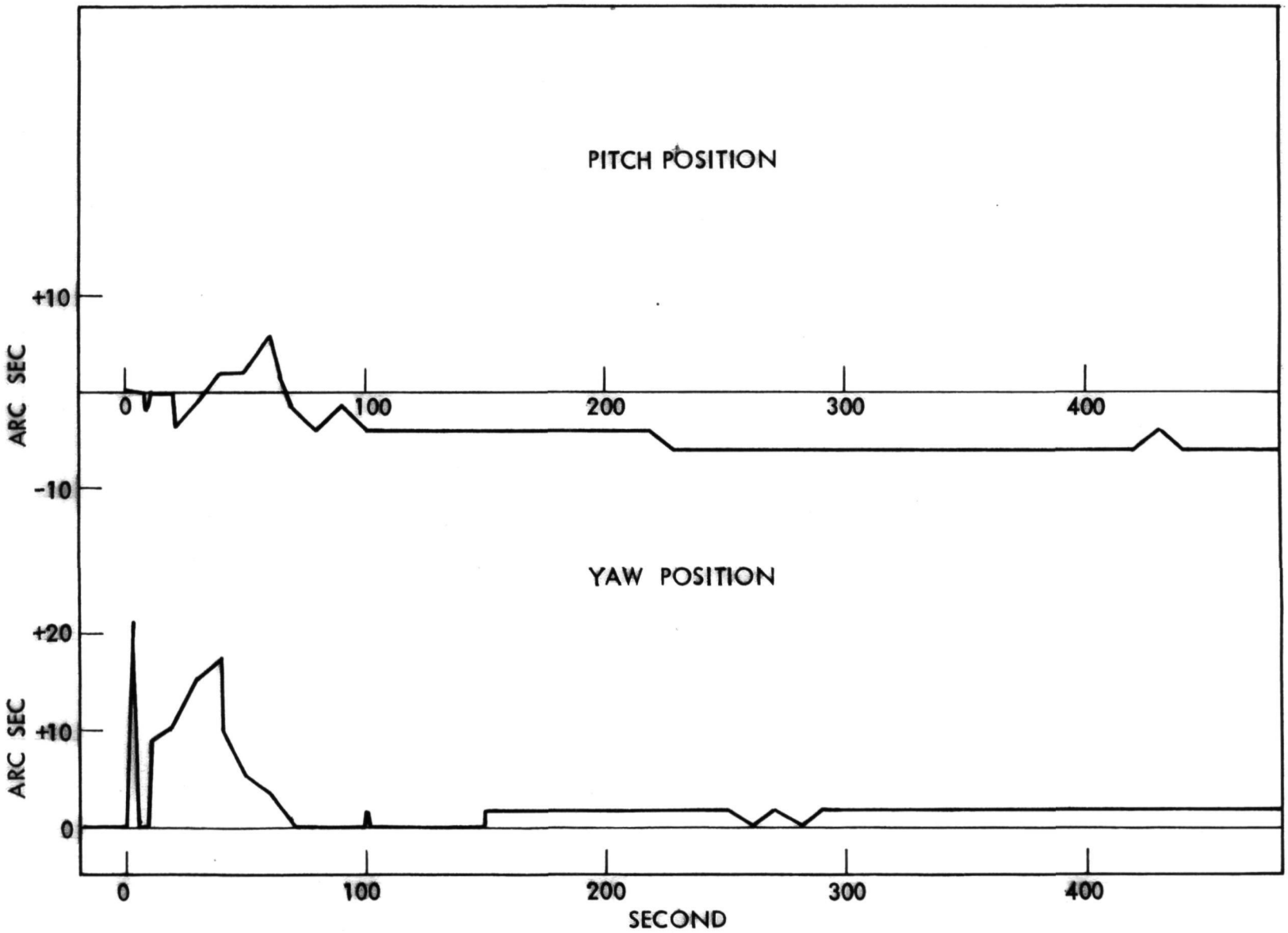

Figure 13 Outputs of the XSST alignment sensor during flight. This measures the relative positions of the XSST mirror and Spectrometer entrance slit and show a return to pre-launch conditions after powered flight at t+70 seconds.

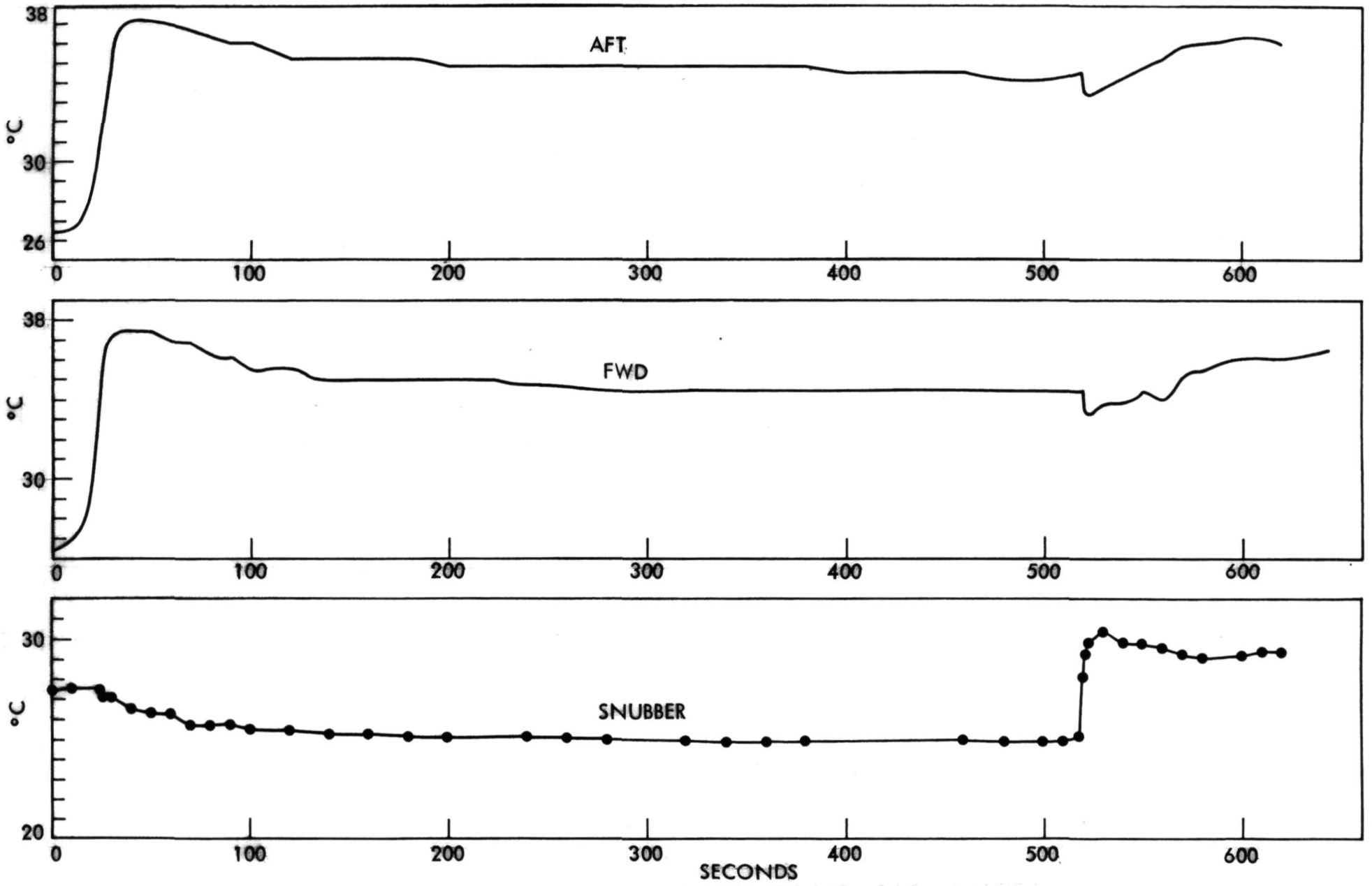

Figure 14 Temperature sensor records. Graphs labeled FWD and AFT are from just inside the skin. The AFT sensor is forward during launch. The SNUBBER plate faces the sun during the pointed phase of the flight. It experienced heating during re-entry when the door failed to close.

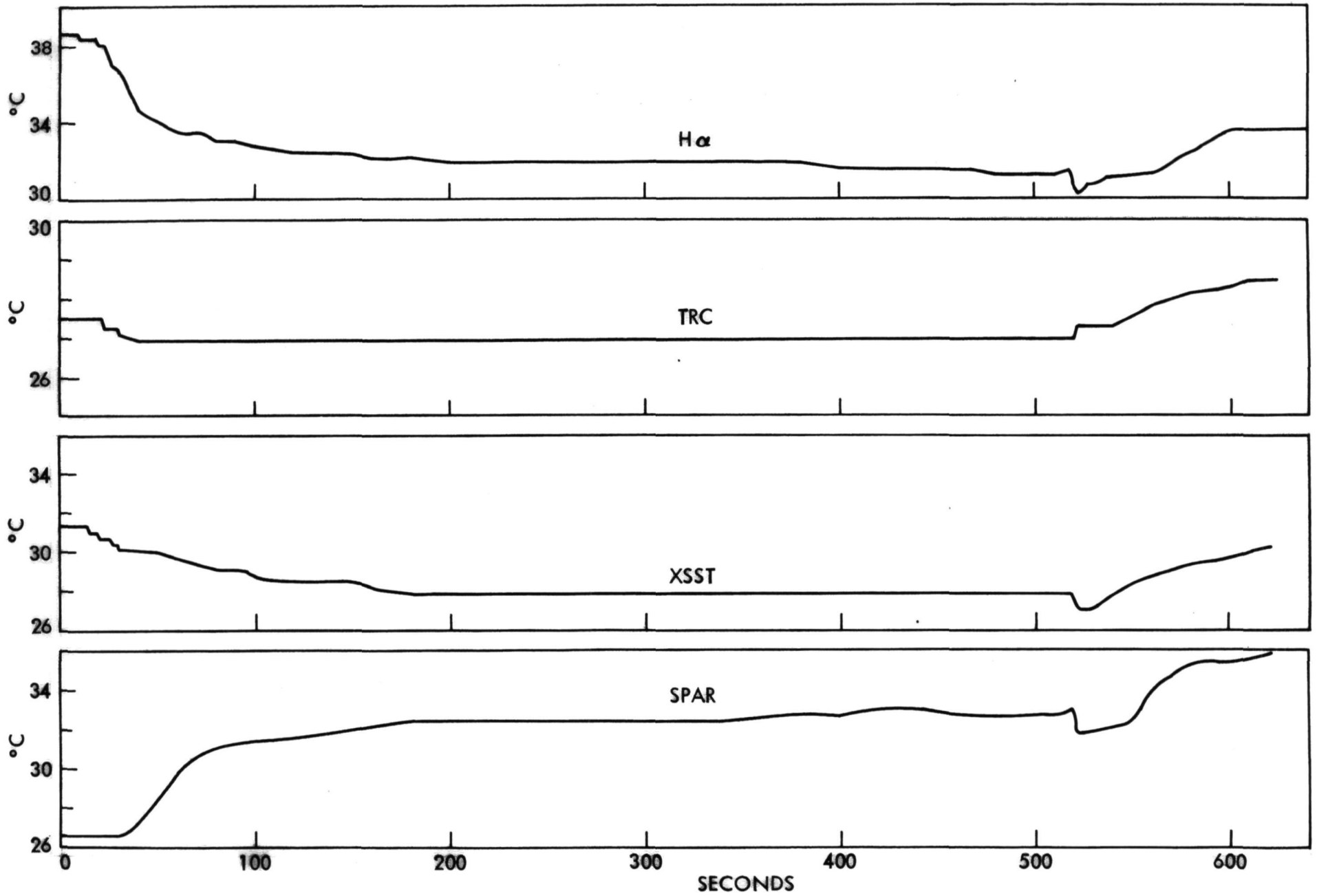

Figure 15 Temperature sensor records. The failure of the H-alpha filter heater is reflected in the fall in temperature and the drift off-band in the filter resulting in loss of contrast. The SPAR temperature monitor is located on the bulkhead connecting the skins to the Spar, while the XSST sensor is in the detector box.

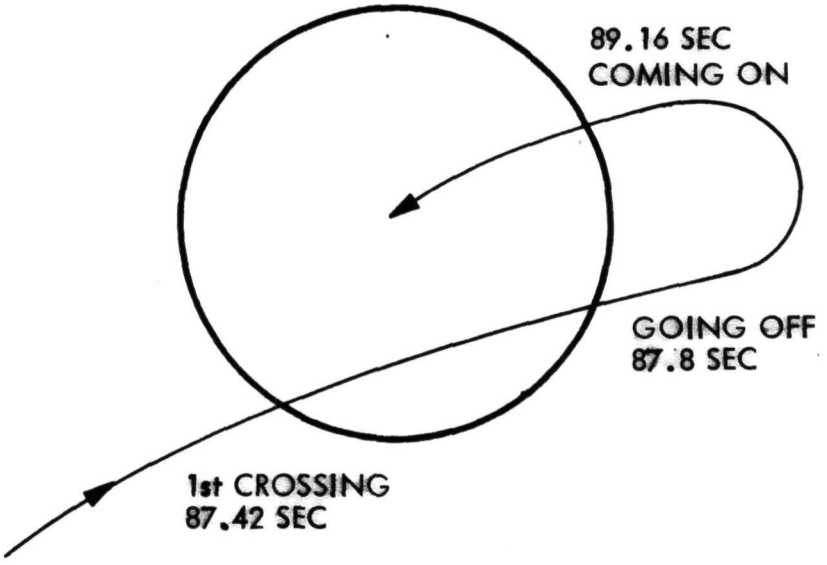

Figure 16 Schematic diagram showing the order in which the limb was crossed early in the flight.

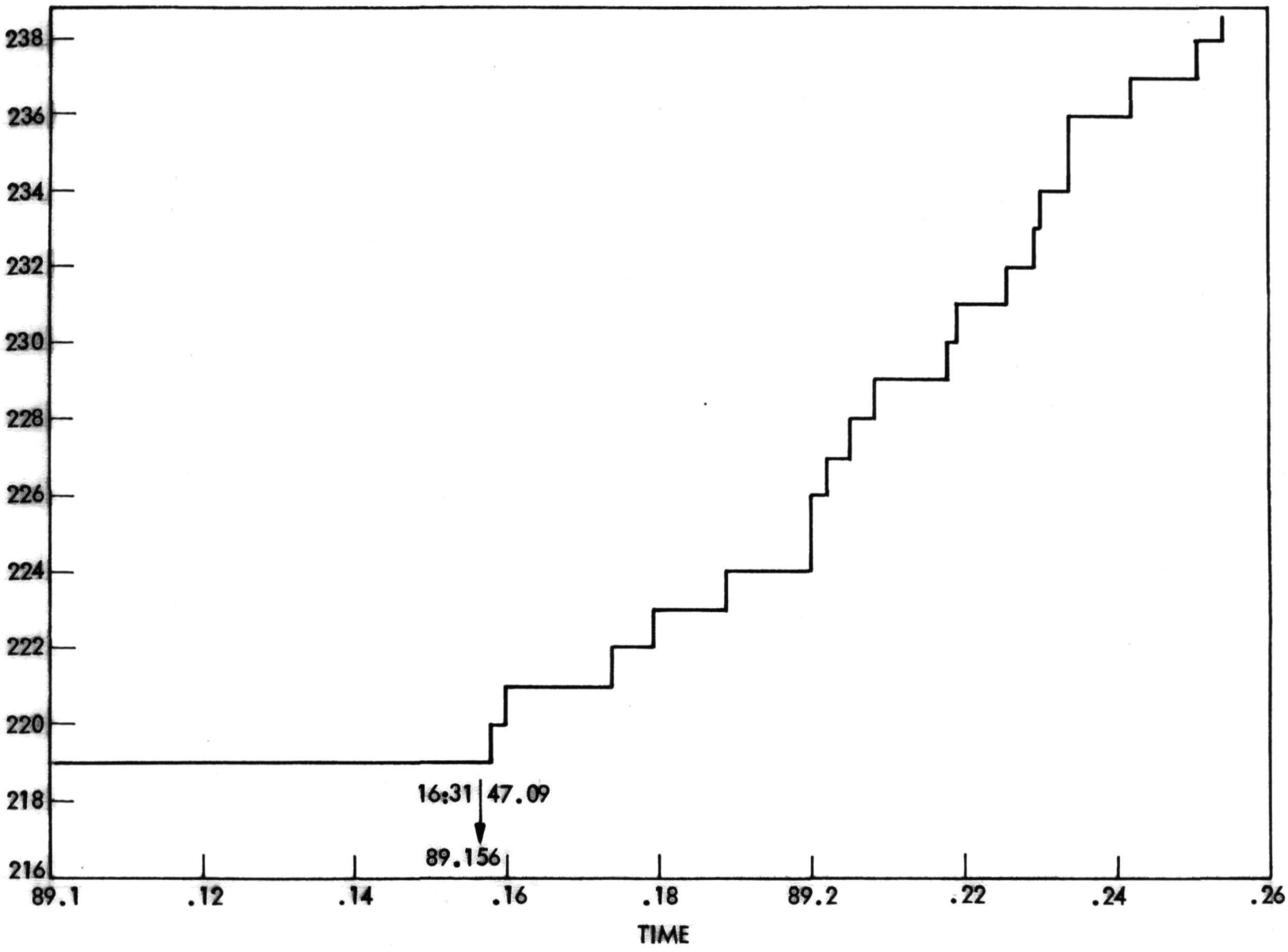

Figure 17 Cumulative CID (central image detector, ultraviolet) counts during the time when the limb was crossed for the third time.

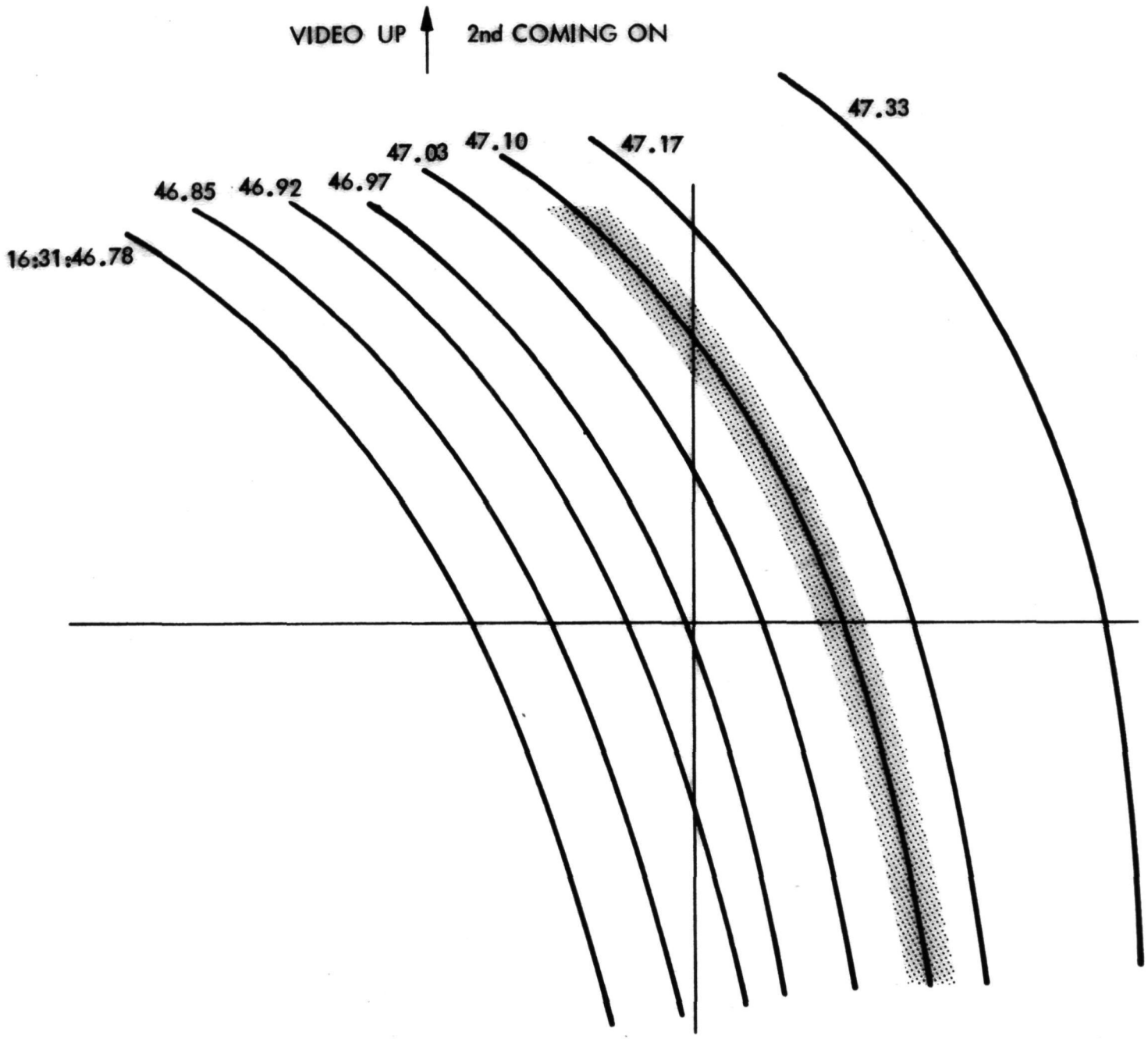

Figure 18. Position of the limb during third limb crossing. These curves were traced from a frame-by frame analysis of the video tape. Times were those displayed on the video monitor in flight.

Fig 19

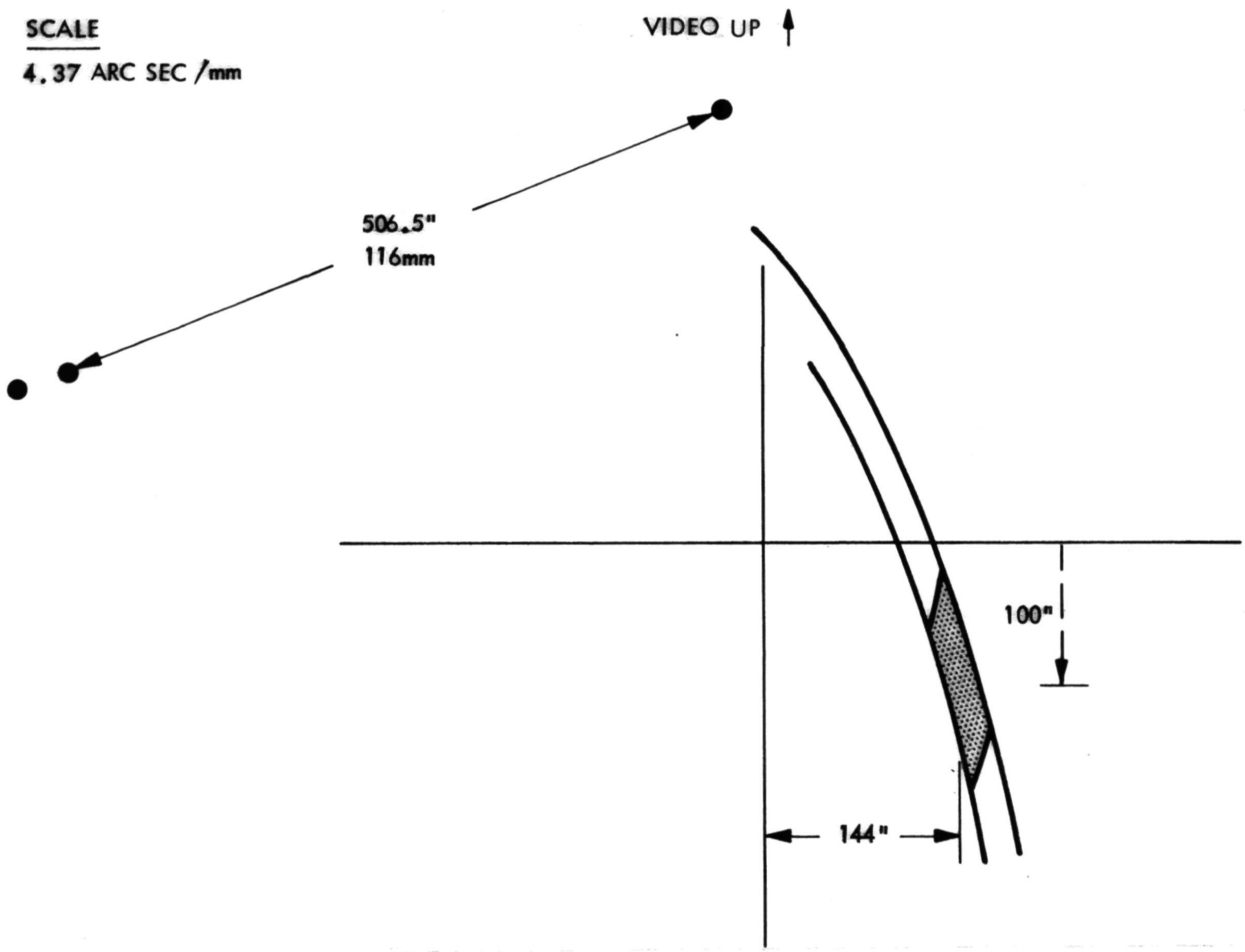

Figure 19 Estimated in-flight pointing offset using only CID limb crossing data.

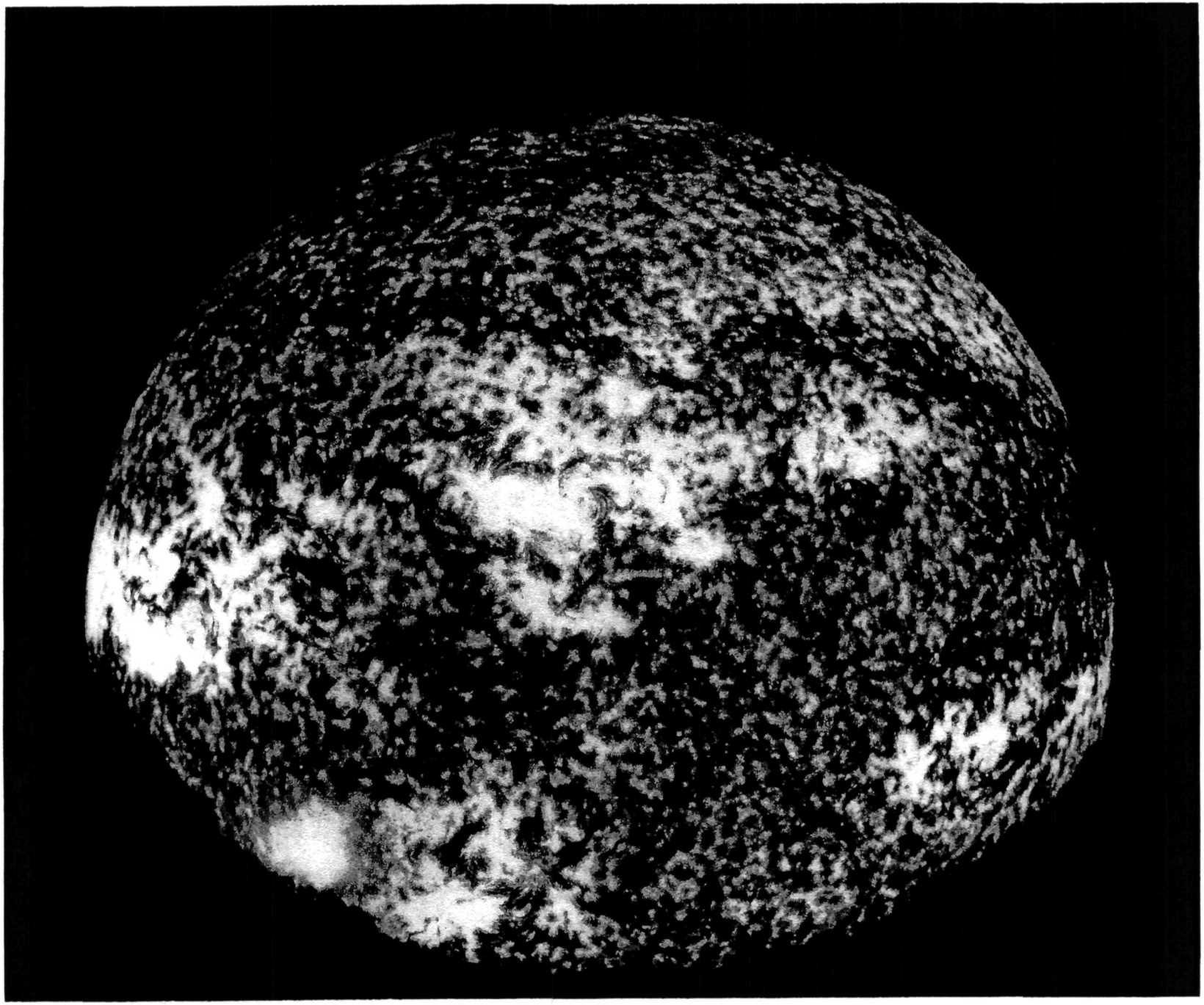

Figure 20. Lyman alpha filtergram from flight 27.032 produced by Transition Region Camera of LPSP.

Reprinted from SPIE Vol. 184—Space Optics—Imaging X-Ray Optics Workshop © 1979 by the Society of Photo-Optical Instrumentation Engineers, Box 10, Bellingham, WA 98225 USA

REFERENCE 1

X-ray spectrometer spectrograph telescope system

E. C. Bruner, Jr.
L. W. Acton
W. A. Brown
S. W. Salat
Lockheed Palo Alto Research Laboratory
3251 Hanover Street
Palo Alto, California 94304

A. Franks
National Physics Laboratory
Teddington, Middlesex
England

G. Schmidtke
W. Schweizer
Institut fur Physikalische
Weltraumforschung
Freiburg, F. R. G.

R. J. Speer
Physics Department
Imperial College
London S.W. 7, England

Abstract

We describe a new sounding rocket payload that has been developed for X-ray spectroscopic studies of the Solar Corona. The instrument incorporates a grazing incidence Rowland mounted grating spectrograph and an extreme off axis paraboloic sector feed system to isolate regions of the sun of order 1 x 10 arc seconds in size. The focal surface of the spectrograph is shared by photographic and photoelectric detection systems, with the latter serving as a part of the rocket pointing system control loop. Fabrication and alignment of the optical system is based on high precision machining and mechanical metrology techniques. The spectrograph covers the 10 to 50 Angstrom interval and has a resolution of 16 milliangstroms in the current version. Modifications planned for future flights will improve the resolution to around 5 milliangstroms, permitting line widths to be measured. The instrument has been developed under the NASA Contract NAS2-9181 and the Lockheed Independent Research Program.

Introduction

This paper will discuss the design and construction of a new rocket payload that has recently been completed for use in the NASA solar physics research program. The payload contains three instruments, the X-ray Spectrometer Spectrograph Telescope, or XSST, an ultraviolet filter camera, and a visible light telescope and filter system. The payload represents the combined efforts of several institutions, including the Lockheed Palo Alto Research Labs (overall design and integration), the Institute fur Physikalische Weltraumforschung of Freiburg, West Germany (Spectrograph slits, Film calibration), the Laboratoire de Physique Stellaire et Planetaire of Paris, France (ultraviolet camera), The National Physical Laboratory, Teddington, England (consultation, X-ray mirror polishing), and the Imperial College, London (Diffraction gratings, calibration).

The program objectives are to measure the physical state and dynamics of the Solar Corona as seen in the 10-50A region, to observe the geometry of the transition zone as seen in the C IV lines at 1548A, and to relate these observations to the underlying structures that are visible in the optical portion of the spectrum. The payload is designed to be launched by a Black Brant V rocket and is to be flown for the first time in June, 1979.

The concept for this instrument package has been previously discussed by Acton, and Catura (1976). The implementation of their concept in terms of hardware is the central subject to be treated here. The design of the Ultraviolet film camera, which was done under the direction of Dr. Roger Bonnet is outside the scope of this discussion.

The elements of the system are shown in Figure 1 and include the 5 meter concave grating X-ray, spectrograph, its collecting mirror, the Ultraviolet Transition Region Camera (or TRC), the H-alpha system, and the structural spar. The spar serves both to maintain mechanical co-alignment of the three optical instruments and the SPARCS sun sensors and to

support them within the rocket airframe. The components of the system will be discussed in detail in the paragraphs to follow. The spectrograph, collecting mirror and transition region camera are mounted on inside surfaces of the spar while the H-alpha system is bolted to the outside. The payload is supported in the rocket by a central bulkhead that connects to the rocket structural cylinders. The cylinders themselves are hermetically sealed, allowing the entire payload to be evacuated. A motor operated shutter assembly at the aperture end of the system is opened after the end of powered flight and then re-sealed just prior to re-entry.

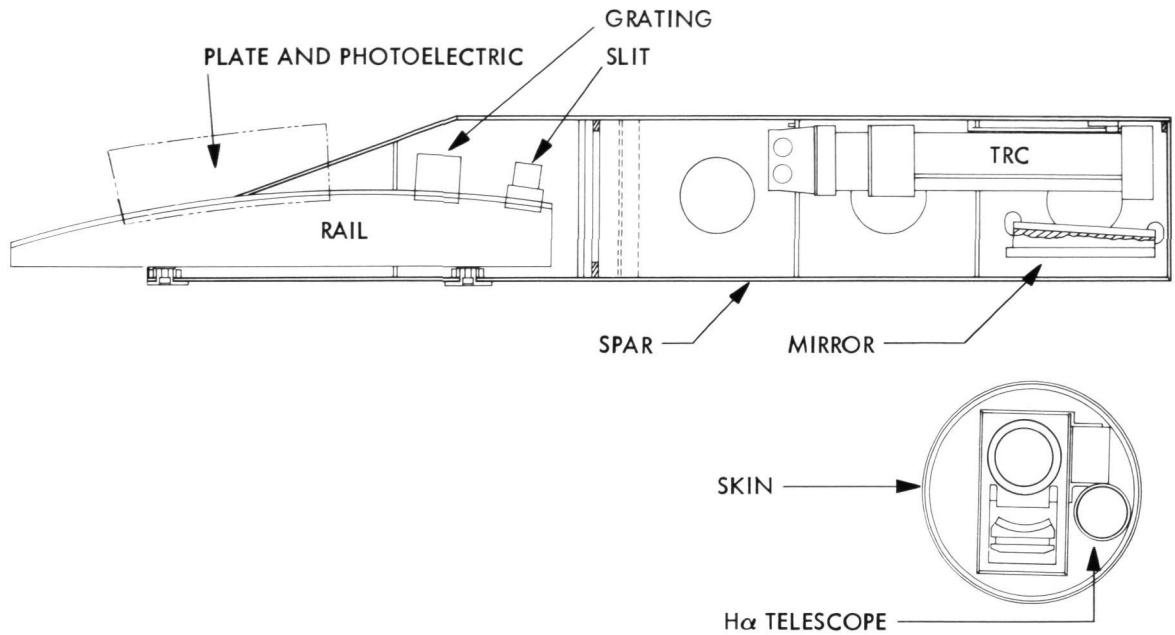

Figure 1: Layout of Solar Rocket Payload showing placement of major instruments in structural spar.

Optical System

The optics of the XSST are shown in Figure 2. X-rays from the sun enter the aperture, striking an off axis parabolic sector mirror at glancing incidence. Following this reflection, they are concentrated on the spectrograph entrance slit at the focus of the paraboloid. Light passing through the slit is incident on a concave grating which, in turn, images the spectrum along the Rowland Circle. The angles of incidence on the collecting mirror and the grating are in the range 2-3 degrees. At these angles, astigmatism in the spectrograph is severe, resulting in astigmatic line lengths of the order of 4 cm. We turn astigmatism somewhat to our advantage in this system by dividing the focal surface into two halves. On one half, we place a photographic plate to record the entire spectrum, while on the other half, an array of discrete photoelectric detectors is used to measure the intensities of a selected set of X-ray lines. It is the dual nature of this detector system that led us to describe the instrument as both a spectrometer and a spectrograph.

The single sector paraboloid was chosen in preference to a two mirror system such as a Wolter Type I or II in order to maximize the system efficiency. Since the single sector lacks coma correction, an extreme off axis section such as ours does not form an image in the usual sense, although rays parallel to the axis of the paraboloid will pass through the focal point. Parallel bundles of rays making an angle with the axis will be mapped onto an arc centered about the axis. The coma is not a serious problem for the spectrograph, since the slit is at the focus, so that light accepted by the slit is restricted to a small portion of the solar surface.

Spectrograph

The X-Ray Spectrograph is a 5 meter grazing incidence instrument fed by an extreme off axis sector of a paraboloid. The spectrograph design is adapted from that of R.J. Speer (1976). The design philosophy of this instrument is based on the premise that optimum optical performance may be achieved without the need for extensive trial and error testing if the design is based on accurate machining and metrology techniques. The heart of the spectrograph is a curved aluminum optical bench on which the slit, grating, and detector

assemblies are mounted. The curved surface is accurately machined to a radius of 245.00 cm which is exactly 50.00 mm less than that of the Rowland Circle. The slit, grating, and detector elements are clamped to the optical bench in mounts designed to hold the components exactly 50 millimeters above the curved surface, thus insuring their accurate placement on the Rowland cylinder. Alignment and focussing of the optical system is carried out in its entirety through reference to mechanical measurements.

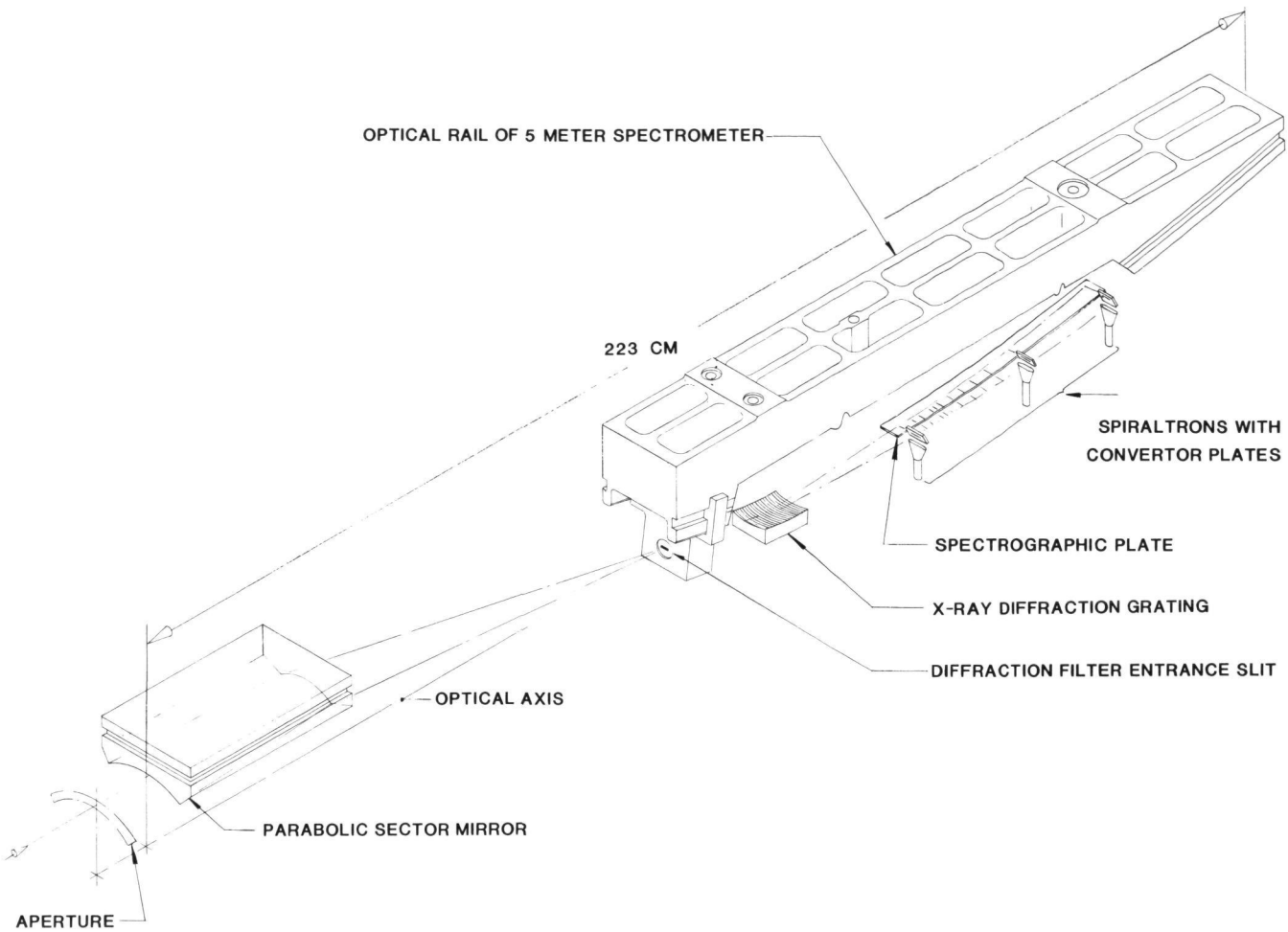

Figure 2.
X-RAY SPECTROMETER-SPECTROGRAPH TELESCOPE

The 5 micron wide by 180 micron long entrance slit incorporates a diffraction filter (Figure 3) in order to reduce the scattered visible light entering the spectrograph. Radiation outside the instruments field of view is collected by a spherical heat rejection mirror mounted just in front of the entrance slit and focussed onto a vee shaped light trap. The slit assembly also carries the light source and detector package for the X-ray telescope alignment system.

Light passing the entrance slit encounters a 632 gr/cm holographically recorded diffraction grating. The angle of incidence is set at 2 degrees, a compromise between photometric efficiency and spectral coverage. The position of the grating is defined by resting its ruled surface on two semi-circular metal rings which have been lapped to conform to the spherical radius.

The focal plane assembly consists of two parts: a discrete channel photoelectric detector assembly, and a photographic plate. The photoelectric assembly includes twelve detector channels, each of which consists of an etched foil exit slit, a photocathode, a Spiraltron (TM) electron multiplier, and a pre-amplifier discriminator for photon counting.

The exit slits are cantilevered from a support outside of the Rowland Circle such that each foil is at right angles to the focussed spectrum rather than lying along the Rowland Circle. This arrangement allows a reasonable tolerance for bending of the foil, which would otherwise need to be unrealistically flat. Settings of the exit slits along the Rowland Circle are made with reference to appropriate combinations of master gage blocks using an electronic height comparator. Setting tolerances are ± 2μ.

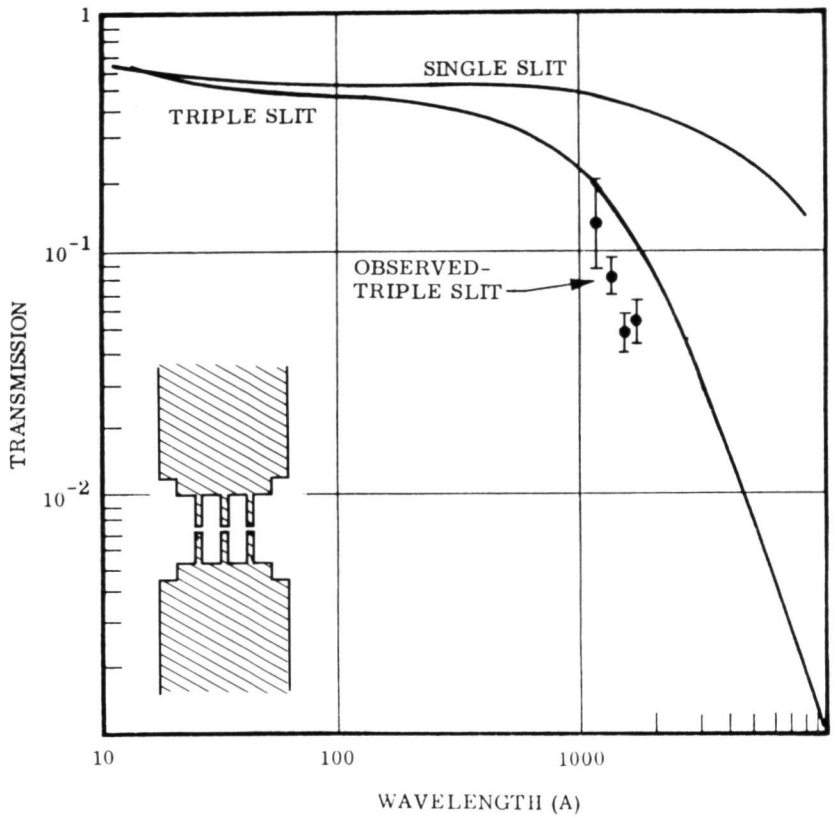

Figure 3. Calculated and observed transmission of IPWF diffraction slit filter sized for first flight of XSST (7μ width).

The zero order of the grating is intercepted by a small mirror placed just ahead of the detector assembly. This mirror deflects the zero order energy into a photomultiplier sensitive in the 1450-1650A range. The signal from this detector is primarily produced by chromospheric and transition zone radiation and may be used to help in the real time location of active regions to be observed with the spectrograph.

Collector Mirror

The spectrograph entrance slit is illuminated by a sector of an off-axis parabola used at an incidence angle of 3°. A sector telescope with extreme grazing angles does not possess an image plane in the usual sense and will focus parallel light to a point only on the axis. Ray bundles making small angles to the axis are severely distorted by coma and will appear as a series of concentric arcs near the focus. Nevertheless, the sector slit combination can usefully limit the field of view as illustrated in Figure 4. Actual performance depends on X-ray scattering properties of the surface, although these will not limit the initial experiments to be done with the payload.

In order to minimize coma, it is necessary to maintain as accurately as possible, the alignment of the axis of the parabola with the entrance slit of the spectrograph. Maintenance of this alignment was the primary motivation for basing the structural system upon a spar concept. Use of the spar together with the thermal control system is expected to hold this alignment to within a few arc seconds. Residual misalignment, whether caused by launch induced temperature gradients or by the difference between the 1 g environment of the lab and the 0 g environment of flight, will be detected by an alignment sensor system. This system consists of an illuminated reticle mounted on the slit assembly, a spherical mirror on the paraboloid cell, and a quadrant detector, again mounted on the slit assembly. When the system is in alignment, the spherical mirror forms an image of the reticle on the

detector such that the four quadrants receive equal illumination. If the telescope axis is displaced by structural distortion, the reticle image will move on the detector and introduce an unbalance among the quadrants. The alignment system is equally sensitive to axis displacement, whether they are produced by translation or rotation of the paraboloid.

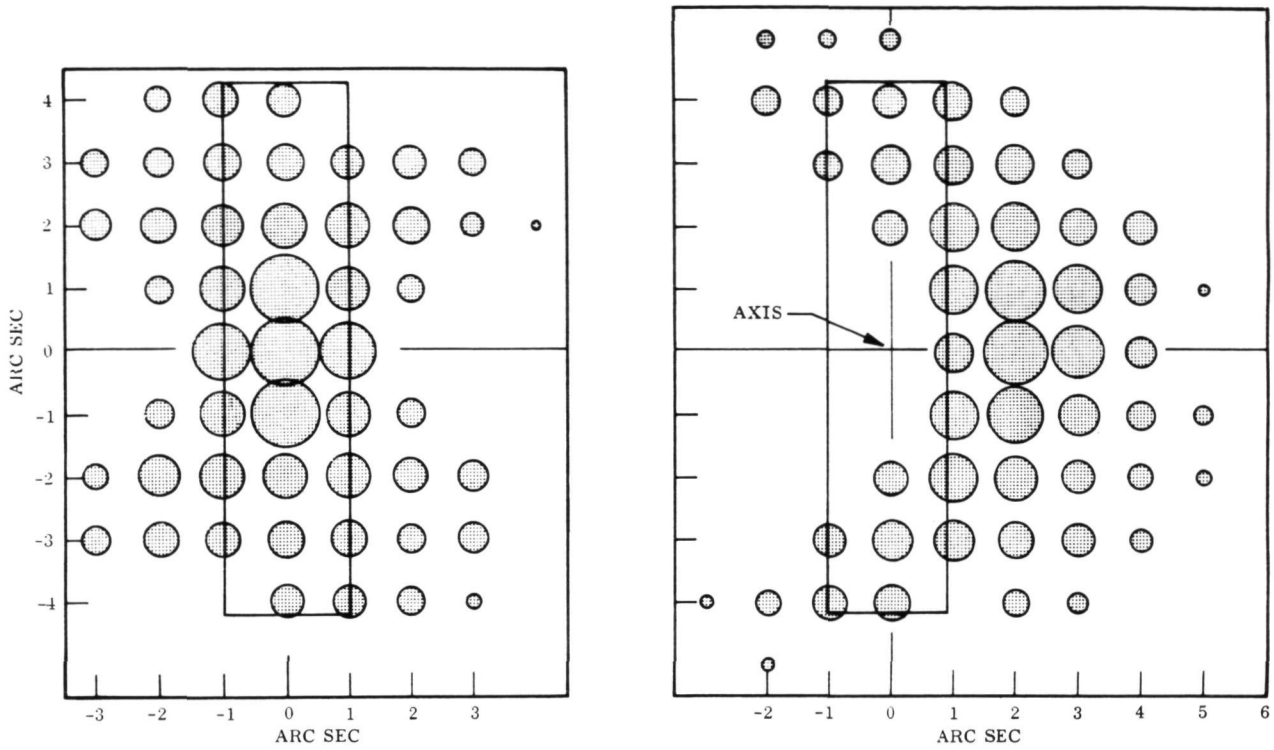

Figure 4. Comparison between nominal and actual angular acceptance zones for XSST: (a) Aligned; (b) Misaligned by 10 μm (circle areas are proportional to instrument sensitivity per unit arc-second squared). These plots are for 10 x 50 μ entrance slit. Actual XSST will use 5 x 10 180 μ slit.

Provision has been made in the mechanical design for the addition of servo actuators to control the paraboloid orientation during flight, although lack of funds prevented implementation of this subsystem for the first flight. Actuators would consist of piezo-electric translators mounted within the mirror cell in place of the mechanical reference pads of the present design. Application of voltages to the translators would produce small position adjustments of the mirror within its cell as needed to correct the alignment.

Structural System

The core of the structural system is a welded aluminum spar, fabricated from 6061-T6 plates. An artificial aging heat treatment was used following weldment to relieve and redistribute stresses and to harden the material in the welded zones. Partial bulkheads are placed at intervals along the length in order to increase the rigidity of the structure. The spectrograph end is tapered for improved access to the detector assemblies. Lapped pads and hardened buttons are provided on the exterior of the spar for use as reference surfaces during metrology and co-alignment of the instruments. Additional machined external surfaces are used as attachment points for the H-alpha system and the X-ray spectrograph.

The spar is attached at its center to a circular bulkhead which is, in turn, fastened to the cylindrical structure of the rocket. The bulkhead is, in effect, a one inch extension of the rocket section. Cylindrical extensions of the rocket structure, attached to the two sides of the bulkhead, serve as the outer housing for the instrument section. Vibrations of the spar within the housing are limited by a snubber system mounted to the telescope end of the spar. The payload is mounted in the inverted (CALROC) configuration with the telescope pointing toward the aft end of the rocket.

The forward end of the payload is hermetically sealed by an aluminum bulkhead while the aft end is fitted with a vacuum tight door assembly that is opened during flight. Evacua-

tion of the payload in the tower is accomplished via an 8" poppet valve in the forward cylinder wall and a pumping station mounted in the launch tower. The pumping system and valve are those designed for the Harvard College Observatory/Center for Astrophysics for use during the ATM CALROC flights. The vacuum door assembly was developed under the direction of Mr. George MacVeigh of the Goddard Space Flight Center.

The Thermal Control System

Thermal control of the payload is needed to suppress temperature gradients in the structural spar which would otherwise introduce alignment errors between the optical elements of the X-ray spectrograph with consequent loss of resolvoing power. Thermal isolation of the instruments is provided by polished aluminum radiation shields mounted just inside the rocket cylinders and by the use of thermal insulation at the joint between the spar and its mounting bulkhead. The temperature of the radiation shield is actively controlled prior to launch so that the instruments will be operated at the temperature at which they were aligned. The active thermal control elements are radiatively rather than conductively coupled to the instruments in order to avoid the introduction of unwanted temperature gradients.

The H-alpha system consists of a 9 cm aperture "Questar" telescope. a reticle assembly, an H-alpha filter assembly, a television camera, and a framing camera. The H-alpha system is mounted on a separate baseplate which is fastened to one of the wide surfaces of the spar. The optical system is arranged as shown in Figure 5. Incident radiation enters the telescope after passing through a field lens, an aperture stop, a telecentric lens, and a narrow band filter set for the 6563 H-alpha line. The filtered beam is divided by a beam splitter cube located behind the filter such that one image falls in the cathode of a television camera and the other onto the film plane of a 35 mm framing camera.

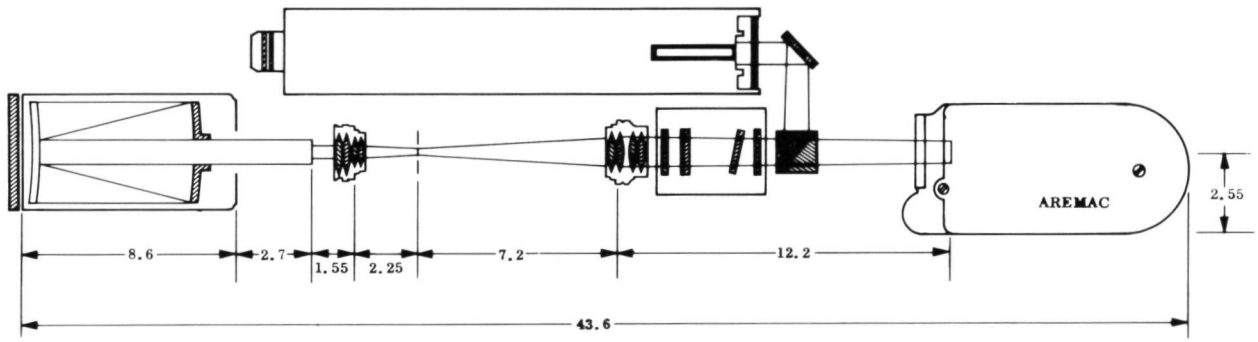

Figure 5. Layout of H-alpha Pointing System with Questar Telescope, 0.75 A bandwidth filter of 6563 A, video and Photographic cameras.

The function of the field lens is to form an image of the telescope aperture on the aperture stop. It suppresses vignetting by returning to the telecentric lens, rays which would otherwise be lost at the edges of the field.

The telecentric lens is placed with its focus at the aperture stop. The effect of this lens is to make the chief ray parallel to the axis of the narrow band filter for every image element of the field. This means that the average angle between the optic axis and the rays making up a given image elements is the same for all image elements in the field with the consequence that the average wavelength of the filter passband is the same for all image elements. The other function of the telecentric lens is to relay the primary telescope image onto the two cameras.

The television image will be used in conjunction with the Automatic SPARCS Command Link (ASCL) for real time pointing of the payload during the flight. The 35 mm framing camera will provide a permanent record of the location of the X-ray field of view with respect to the chromospheric network for use in data analysis.

Expected Performance

The projected field of view of the XSST on the sun is of the order of 1 x 30 seconds of arc. Using this information and available data on mirror reflectivity, grating efficiency, etc., it is possible to estimate the sensitivity and resolution performance of the instru-

ment for solar observations.

The results of this analysis are summarized in Table 1 for several important soft X-ray lines in the 10-50 Å region spanning the temperature range 1 - 5 x 10^6 K. The spectral resolution of the XSST is approximately 13 mÅ in the first order.

For the photoelectric portion (λ < 40 Å) of the XRST we have examined the instrument sensitivity by computing for each line the intensity I_r, required to register a counting rate, R, of 10 counts/sec. Similarly, for the photographic section we have derived the intensities, I_d, required to produce an exposure, E, of 3.5 x 10^6 photons/cm^2 on the plate in 60 sec. For normal Kodak 101 plates this exposure will produce a photographic density of 0.2.

The derived "adequate intensities" I_r and I_d (please note that these are in no sense limiting sensitivities) are expressed in terms of solar conditions in 3 different ways. Finally, for four lines we give the range of intensities observed in 3 separate active regions by experiments flown by us on 11 June and 19 December 1973.

Table 1. Summary of XRST Performance

λ (A)	Ion	(a) T_m (10^6K)	(b) $-\log_{10} F_m$	(c) $\Delta\lambda_D$ (mÅ)	(d) I_r	(e) I_d	(f) I_{AR}
12.13	Ne X	5	43.6	4.3	75	158	
13.45	Ne IX	3	43.8	3.7	56	133	13 - 69
15.01	Fe XVII	5	42.2	3.2	49	113	46 -274
18.97	O VIII	3	42.2	5.9	61	83	27 -165
21.60	O VII	2	42.4	5.3	56	76	
28.79	N VII	2	42.9	7.0	39	64	
33.74	C VI	1.5	42.1	8.0	30	59	
40.27	C V	0.9	42.5	7.9	24	59	

Footnotes

a Temperature of peak emissivity.
b Line flux at earth from solar plasma at T_m photons cm^{-2} sec^{-1} (unit emission measure)$^{-1}$.
c Full width at half maximum of Doppler profile at T_m.
d Intensity photons cm^{-2} sec^{-1} arcsec^{-2} required to obtain photoelectric counting rate of 10 c/s from XRST.
e Intensity photons cm^{-2} sec^{-1} arcsec^{-2} required to obtain photographic density of 0.2 in a 60 second exposure.
f Range of intensities observed in 3 separate active regions in June and December 1973.

Operation of the instruments during a sounding rocket flight is based upon use of the Lockheed developed SPARCS attitude control system and the automated SPARCS command link (ASCL). SPARCS is a gas operated reaction pointing system designed for solar physics use. Attitude signals for the system are derived from photoelectric detectors that sense the relative position of the sun and from a magnetometer that provides roll information. Offset pointing by introducing an electrical bias into the control loops, either by ground command or from an on-board raster generator. The automated SPARCS Command Link is a computer based control terminal that can receive and evaluate the real time telemetry signal and send commands to the payload, either to alter the pointing or to operate the subsystems in the instrument.

The flight of our instrument will include the following phases. Prior to launch, the payload will be preconditioned at high vacuum for several hours in the launch tower. During this time, the active thermal shroud will be controlled to adjust the payload to the temperature of optimum focus. At launch, the thermal system is disconnected and thermal control is passive for both the powered and unpowered portions of the flight. Following burnout of the Black Brant sustainer motor, the payload and sustainer are separated, the vacuum shutter opened, and the pointing system is enabled for initial acquisition of the sun.

Once solar pointing has been acquired, the ASCL comes into play. The television image from the H-alpha system is transmitted to the ASCL control room and displayed to the experimenter on a monitor. The experimenter selects the general region to be observed, using a joystick controlled fiducial on the TV image. The ASCL computer computes the pointing offset needed to center the target and automatically formats and transmits the appropriate commands to the pointing system.

Following target selection, is a two phase bright point search. The first phase is relatively coarse and identifies the center for a second finer search. Both search patterns are produced by the raster generator which is carried on board. During the searchs, the

ASCL computer continuously monitors the data from the X-ray detectors. Numerical images of the raster pattern are built up in the computer memory as the scan proceeds and may be searched for maxima after the scan is complete. Three such images are formed, one from the intensity of the strongest X-ray line, one from a sum of 3 strong lines, and one from the central image detector. After each scan, the ASCL operator selects which of the images is to be used for bright point selection. Manual overrides are available if desired by the operator. When bright point selection is complete, the computer again formats and transmits the pointing commands. The final pointing position is taken as the target for exposure of the photographic plate.

Summary

Our objectives in developing the system we have just described are twofold: First, to extend the state of the art of space borne high resolution spectroscopic instrumentation into the technically difficult spectral region between 20 and 50 Angstroms, and second, to explore this spectral region on the sun. We expect first flight to produce the most highly resolved solar spectrum yet recorded in this spectral range. Modifications planned for future flights will allow the measurement of X-ray line profiles.

The design and construction of an optical instrument based on high accuracy machining and metrology has proved to be a challenging engineering problem, though by no means an insurmountable one. The technique has several advantages. The final alignment can be carried out in ambient laboratory conditions, avoiding a tedious series of trial exposures in a vacuum system. Rechecking of the alignment can be done in the field following system level environmental tests, again without resort to vacuum. Finally, since the construction and alignment of the instrument is based on accurate mechanical measurements, we expect to be able to measure absolute wavelengths of the observed lines with a high degree of confidence, and to derive absolute doppler velocities.

The first flight of the instrument is scheduled for July, 1979 at the White Sands Missile Range. We are hopeful that it will prove to be a valuable new approach in the study of high temperature astrophysical plasmas.

Acknowledgements

We are pleased to recognize the participation of a number of individuals who have made valuable contributions to this program. The diffraction gratings were made at the National Physical Laboratory, Teddington, and calibrated by Grating Measurements, Ltd, London. Fabrication of the X-ray collecting mirror was done by Ion Tech, Ltd., of Teddington, England and measurements of its surface contour and figure were done at the National Physical Laboratories. We are pleased to acknowledge the contribution to these efforts of Dr. R. Johnson, Dr. M. Stedman, Mr. V.W. Stanley, and Dr. Brian Gayle. Design and construction of the electronic subsystem was done at Lockheed by Mr. R. Caravalho. Finally, we recognize and express our appreciation for the critical role played by the Moore Special Tool Company of Bridgeport, Connecticut, who performed the high accuracy finish machining and metrology of the curved optical bench of the spectrograph. Mr. Salat was assisted in the mechanical design by J. Vieira and in the Optical and Mechanical design of the H-alpha system by T. Pope and R. Reeves. This work was supported by NASA and by the Lockheed Independent Research Program.

References

1. Acton, L.W. and Catura, R.C., "Instrumentation for Solar and Cosmic X-Ray Spectroscopy", Space Science Instrumentation, 2, 445 (1976).
2. Speer, R.J., "The X-Ray Diffraction Grating", Space Science Instrumentation, 2, 463, (1976).

Reprinted from SPIE Vol. 184—Space Optics—Imaging X-Ray Optics Workshop © 1979 by the Society of Photo-Optical Instrumentation Engineers, Box 10, Bellingham, WA 98225 USA

REFERENCE 2

Paraboloidal x-ray telescope mirror for solar coronal spectroscopy

W. A. Brown
E. C. Bruner, Jr.
L. W. Acton
Lockheed Palo Alto Research Laboratory
3251 Hanover Street
Palo Alto, California 94304

A. Franks
M. Stedman
National Physical Laboratory
Teddington, Middlesex, England

R. J. Speer
Physics Department
Imperial College of Science & Technology
Prince Consort Road
London SW7 2BZ, England

Abstract

The telescope mirror for the X-Ray Spectrograph Spectrometer Telescope System is a sixty degree sector of an extreme off-axis paraboloid of revolution. It was designed fo focus a coronal region 1 by 10 arc seconds in size on the entrance slit of the spectrometer after reflection from the gold surface at a glancing angle of about 2.9 degrees. This paper discusses the design, manufacture, and metrology of the mirror, the methods of precision mechanical metrology used to focus the system, the mounting system which serves to locate the mirror and has proven itself through several vibration tests, and the results of reflection efficiency measurements at 8 and 44 Angstroms, and alignment tolerances and ray trace analysis of the effects of misalignment. The mirror was developed under NASA Contract NAS2-9181.

Introduction

The paraboloidal X-ray telescope mirror described here is the telescope of the XSST (X-ray spectrometer-spectrograph telescope), an advanced rocket borne instrument which provides soft X-ray diagnostics of the solar corona. The mirror is designed to be mated with the spectrometer in such a way that the entrance slit of the spectrometer defines a one by ten arc second portion of the corona. This report describes the design of the mirror to meet the special requirements imposed by the solar research anticipated, and presents results of measurements made at NPL, and Imperial College. Mounting the mirror in the rocket payload and alignment by mechanical metrology are discussed, results of Monte Carlo type calculations which predict its field of view are given and reflectivity measurements at Imperial College are displayed.

Design of the XSST Mirror

The configuration of the XSST telescope mirror is determined by its relation to the XSST instrument itself, which is described in the preceding paper by Bruner, et. al. in these proceedings. Briefly, the goal of the XSST program is to obtain both photographic and photoelectric spectra of small, well defined regions in the solar corona in the 10 to 50 Angstrom wavelength interval. The instrument is the major component of a sounding rocket payload of seventeen inch diameter and two meter length. The special requirements of spectroscopy at soft X-ray wavelengths include reflection at glancing incidence and minimizing the number of reflections. A five meter Rowland circle diameter was chosen for the spectrometer with angle of grazing incidence on the grating of two degrees at the grating pole. Paraboloidal telescopes of the type employed here were described by Giacconi and Rossi[1]. Such a device usually consists of a surface of revolution of a parabolic arc rotated 360 degrees about the x axis where the equation of the parabola is $y^2 = 2px + p^2$. This type of telescope is also referred to as the Wolter Type 0 after Wolter's[2] classification of glancing incidence mirror systems for X-ray microscopy and other applications. This design attempts to maximize the collecting area useable by a paraboloidal telescope coupled with a spectrometer at the entrance slit. The design selected is a 60 degree segment of the paraboloid of revolution about the X-axis. Figure 1 is a sketch of the layout and specifications are given in Table I.

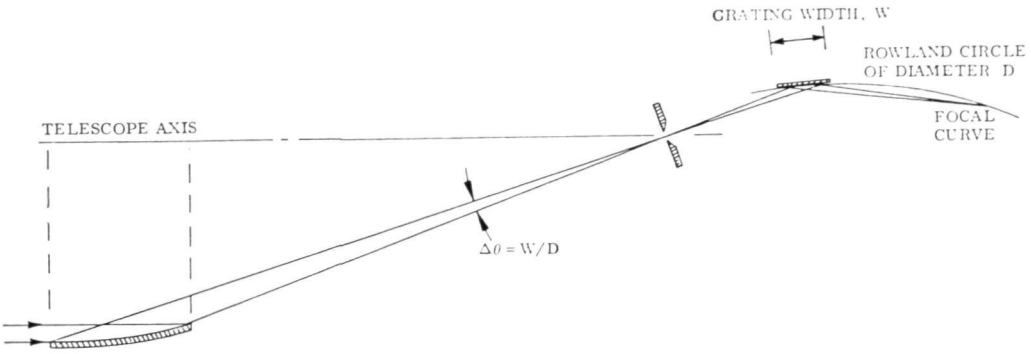

Figure 1. XSST Geometry: Section through paraboloidal mirror, and Spectrometer. $\Delta\theta \simeq 0.5^{\circ}$; Useful Grating Width ≃ 4 cm; D = 5 meters.

Table 1. XSST Mirror Specifications

		Tolerance
Finished length parallel to axis	21 cm	± 0.25 mm
Finished width	10.4 cm	± 0.25 mm
Radius of revolution at mirror front	10.4 cm	± 2.0 mm
Axial distance from mirror front to focus	121.5 cm	± 5 mm
Equation of surface	$y^2 = 2p(x + p/2)$	
Implied value and tolerance of p	0.5348	± 0.02 mm
Accuracy of figure (departure from a true paraboloid)	$\lambda/5$ at 5000Å to within 3 mm of sides and 10 mm of ends	
Micro ripple design goal	10Å p-p	
Slope error	≤ 1 arc sec	
Number of mechanical reference surfaces	6	
Nominal size of reference surface	5 mm	

Metrology and Alignment of the Mirror

Alignment of the telescope mirror in the XSST is done by precision mechanical metrology. This approach was undertaken because of the necessity to hold small tolerances and the difficulty of optical alignment with this system. The paraboloidal surface is employed at a grazing angle of 2.8 degrees near its center, so that imaging is very poor for points off axis. A point at infinity is imaged as a point at the focus, but an off axis point is imaged as a circle, or in the case of the 60 degree sector used here, a circular arc. An additional problem encountered in aligning the paraboloidal telescope in the XSST is the unusual three jawed entrance slit buried inside a relatively massive assembly. This slit, whose aperture is 5 by 150 microns in size, transmits very little light, and in fact its function is the supression of visible light. Diffraction effects at visible wavelengths also add to the difficulty of optical alignment to the desired tolerance. For these reasons the figure of the mirror was carefully determined by mechanical metrology and referenced to surfaces on the blank that could be used in a mechanical alignment scheme.

Figure 2 shows a model of the mirror blank in the special holder described below. Precision metrology of the mirror was undertaken at National Physical Laboratory, Teddington, England with the aid of the S.G. Trioptic measuring machine. The mirror was set face up on the machine and was adjusted to align the flange and side face to the machine axes X_m, Y_m, Z_m. A vertical ball-ended probe was used as a fiducial indicator in setting the vertical motion of the machine. Readings on the mirror surface were taken at 30 grid points. Readings on the ledge were taken using slip gauges to raise the measurement point to a convenient height. The vertical-face pads were also measured with the vertical probe, by measuring at five or six points on the surface of a precision 3/4" roller held in contact with the pad being measured. A circle-fitting procedure enabled the co-ordinates of the roller centre to be found, and hence those of the contact point on the pad.

The six sets of five readings on the circular arcs were each fitted by a least squares procedure which minimised Σd^2 in the radial direction. The centre 3 points were weighted 2:1 relative to the outer points which were believed to be slightly less reliable due to contact on a slope. The average deviation from the fitted circles was about 0.8μm.

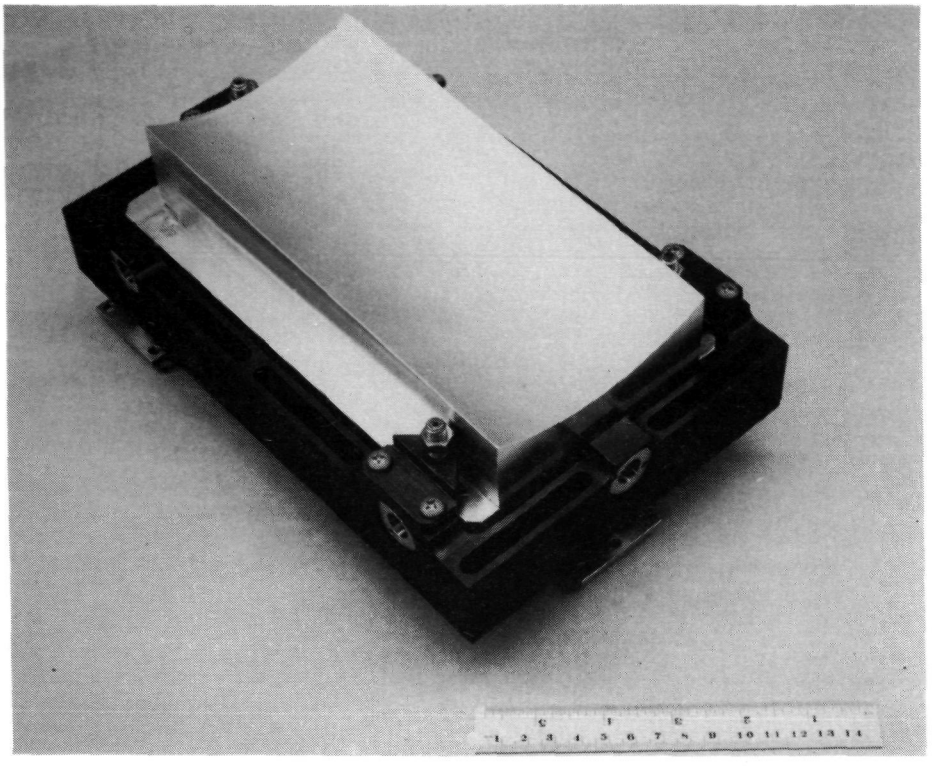

Figure 2. Mirror Cell with Model Mirror.

Regression analyses of the co-ordinates of the centres of the fitted circles were made against the axial position X, to estimate the most probable direction of the axis of revolution. Each fitted circle provided a co-ordinate for the probe centre, and was corrected using the probe radius and a theoretical mirror slope to provide 6 co-ordinate pairs characterizing the mean parabolic generatore. A parabola was fitted to these points, with the constraint that the apex of the parabola must lie on the estimated axis of revolution. The best fit obtained gave $\Sigma d^2 = 0.62\ \mu m^2$. The co-ordinates of the focus were calculated, and finally all the co-ordinates of the reference points and paraboloid parameters were translated and rotated to conform to axes referred directly to the reference points. The original measurements were reproducible to about 1μm although readings were taken to 0.1μm.

It must be emphasised that the paraboloid chosen to fit best gave the lowest value of Σd^2, but many others would have given acceptable values of Σd^2. In a sense this reflects the range of focal positions available with an acceptable performance.

The profile measuring machine was used to measure the profile of a shallow generator relative to a chord, and is primarily designed for rapid and accurate measurement during production. One of the last scans taken before the final polishing of the mirror shows average deviation of less than 0.2μm. The results indicate that the profile is of excellent accuracy. Note that although the p-value (5.2774 mm) differs slightly from that derived from the 3-axis measurements, this may be partly due to the final polishing and is in any case not regarded as significant.

Twyman-Green Interferometric Test

The mirror was set up so that the nearly spherical wavefronts returned from the mirror would be compared with those returned from an accurate spherical reference mirror. The essentially straight and uniformly spaced fringes indicated that the wavefronts were very close to spherical, and were simply tilted with respect to the reference wavefront. It was possible to virtually "fluff out" the fringes completely, although this condition is not easy to photograph. The junctions of the mirror and side blocking pieces could be seen clearly, and accuracy of figure was seen to extend over virtually the whole of the mirror.

Figure 2 shows the special mounting fixture for the paraboloidal mirror. It is a shallow rectangular aluminum box which is fastened to the instrument structural member (Spar) by three steel bolts and spacers which transfer the plane of reference for the mirror through the wall of the Spar to the granite table used in the alignment. (An aluminum model of the mirror is shown in the photograph). The mirror is held in the mount by six clamps, three of which act on the ledge around the blank to define a plane and three of which act through the body of the blank to prevent rotation. Each clamp consists of two parts, a pad and an adjustable screw. The pad is a hardened steel hemisphere in a convex socket. Opposing this is spring loaded adjustment screw which contacts the blank through a flat steel pad. This mounting system has three features which are important for holding a mirror stably, in a precise position, yet allowing it to withstand vibration associated with space flight qualification and launch. Precision positioning of the mirror in the holder is accomplished by lapping the flat surfaces of the hemispherical balls. The lapped surfaces are mirror smooth and the surfaces of the blank which are contacted are also smooth. While this insures repeatable measurement, it was found that a tiny amount of teflon lubricant is needed to prevent wringing together of the parts. Under vibration, the clamps allow movement of the mirror against the light resistance of the springs up to an amplitude of about three mils (76 microns). This feature prevents distortion of the mirror by the mount, yet the small vibrational amplitude insures that g-forces at the limits of travel are low. (The mounting concept is derived from a design by W.G. Fastie).

Alignment of the paraboloidal telescope mirror with respect to the XSST spectrometer is performed by mechanical metrology. The instrument is supported on a granite surface plate under controlled conditions and a three dimensional coordinate system is established. The most critical part of this procedure is the placement of the mirror so that its focal point is at, or very near, the spectrometer entrance slit, since imaging deteriorates rapidly as one moves away from this point. (Ray trace resuls given below illustrate this effect). Since the axis and focal point of the paraboloid are known with respect to the reference surfaces on the mirror, we proceed by locating their position to half micron precision, and lapping the steel hemisphere support balls to achieve alignment. It should be noted that while the tolerance for locating the focal point with respect to the entrance slit is about twenty five microns (0.001 inch) the one meter focal length of the mirror and fifteen centimeter length over which measurements are made, dictate ten times smaller tolerance in the mirror mount settings.

Measurements of the mirror position before and after vibration tests in the fully assembled rocket payload, showed that the mount had performed very well and contributed no detectable misalignment.

Ray Trace Predictions of Field of View

The field of view of the XSST on the sun is determined by the alignment of the mirror, the size of the spectrometer entrance slit, and the portion of the spectrometer astigmatic line length from which energy is collected. This latter point is important because longitudinal strips on the surface of the mirror map onto intervals in each spectral line, a situation which arises when extreme angle of glancing incidence are employed in both mirror and grating. Figure 3 shows schematically the paraboloidal mirror, entrance slit (S), concave diffraction grating (G), spectrographic plate and photoelectric detector slits. The shallow curvature (5 meter radius) of the grating produces negligible bending of the rays in the plane represented by the drawing. A monte carlo type ray trace program for X-ray

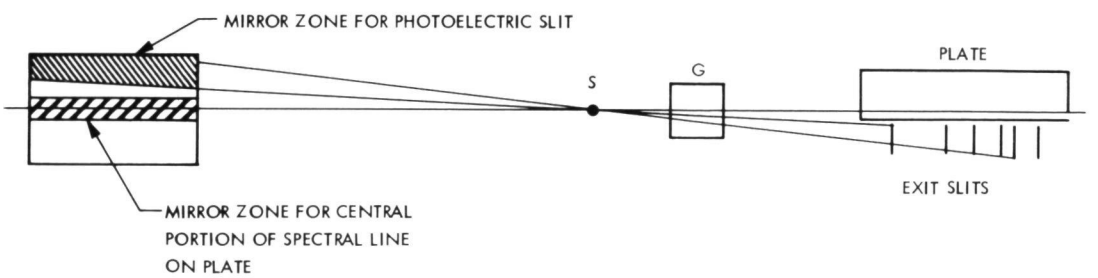

Figure 3. Schematic showing relation between zones on mirror and Detector Positions on Astigmatic Spectral lines.

optics was used to predict fields of view for the particular parameters chosen, and to study the effects of the unavoidable misalignments that can arise due to residual thermal stress. The ray trace program distributes rays at random over the selected portion of the mirror entrance annulus. A matrix of angular offsets from the axis of revolution of the mirror is formed and those rays originating in each angular interval are reflected from the mirror and followed through the entrance slit of the spectrometer. Figure 4 is a selection of these angular matrices for two conditions of instrument internal alignment, and three detector configurations.

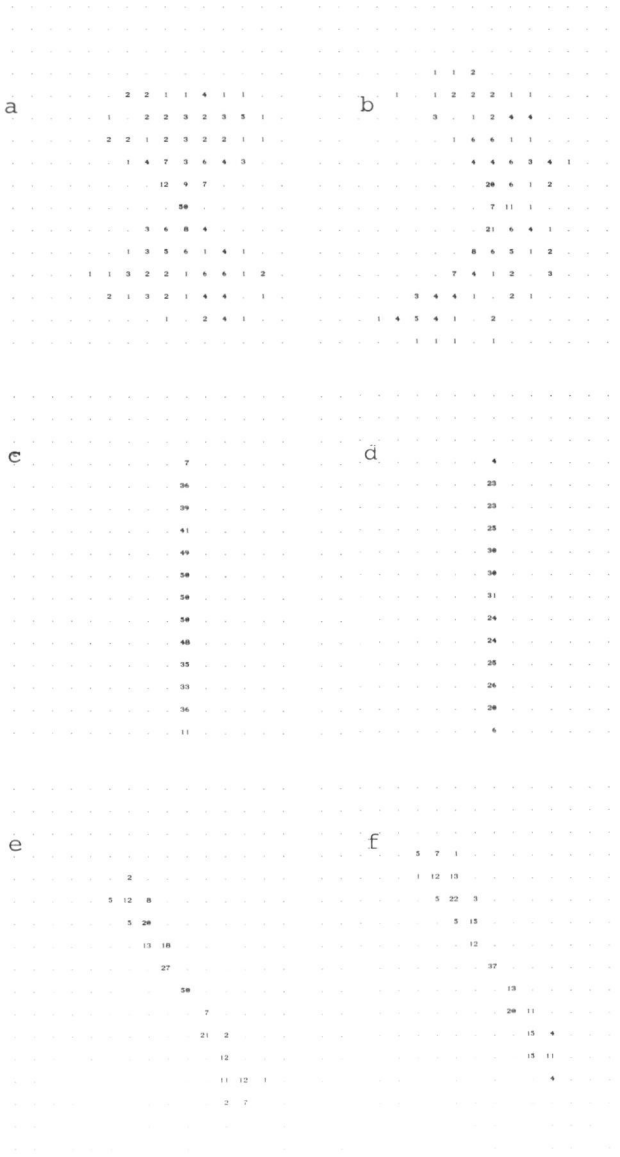

Figure 4. Patterns on Sun seen by combinations of mirror zone and 150 x 5μ entrance slit.

Each of the six matrices in Figure 4 is an array of 2.5 by 2.5 arc second cells representing the collection efficiency of the instrument from such annular regions on the sun. Figures 4a and b represent the pattern on the sun seen by the entire mirror and the 5 by 150 micron entrance slit. In 4a the instrument is perfectly aligned and in 4b the focal point of the mirror is offset 30 microns (5.25 arc seconds) from the nominal position. The dumbbell shape of the zone on the sun from which energy is collected by the full mirror, is related to the length of the entrance slit, but no detecting element makes use of the full aperture of the paraboloidal mirror. The spectrographic plate is fed by light collected by

slightly more than half the mirror and longitudinal zones on the mirror can be identified with segments of the astigmatic lines. The central two millimeters of a spectral line is fed by a narrow 2.8 degree zone of the 60 degree mirror sector and the angular region on the sun from which this zone collects energy is shown in Figures 4c and d. As above, the map on the right (4d) shows performance when a 30 micron offset is introduced in a direction orthogonal to the slit long axis. In this case, little change is apparent, in contrast to the distortion seen in 4b. The twelve photoelectric detector exit slits in the XSST collect energy from a ten degree zone of the mirror and Figures 4e and f show the solar zones seen by one of these photoelectric detectors.

Reflectivity Measurements and Interferometric Examination

Measurements were made at the Blackett Laboratory, Imperial College of Science and Technology, to assess the accuracy of the mirror figure and to obtain X-ray reflection efficiency at two wavelengths. These measurements were made over six months after the mirror was manufactured and had survived several vibration excercises. It had also been installed in the XSST rocket payload, which was evacuated more than once.

The XSST mirror was installed in the X-ray test facility at Imperial College and an essentially parallel X-ray beam irradiated the central part of the mirror at and near a 2.8^{o} grazing angle. To normalize the measurements and confirm source stability, the mirror could be completely retracted from the X-ray beam. Six independent measurements were made at 8.3 and 44 Angstroms over an 8 day period in March, 1979. Figure 5 gives, as open circles, the results of the reflectivity measurements, compared with data on similar surfaces from Hendrick [4] and Ershov et. al.[3].

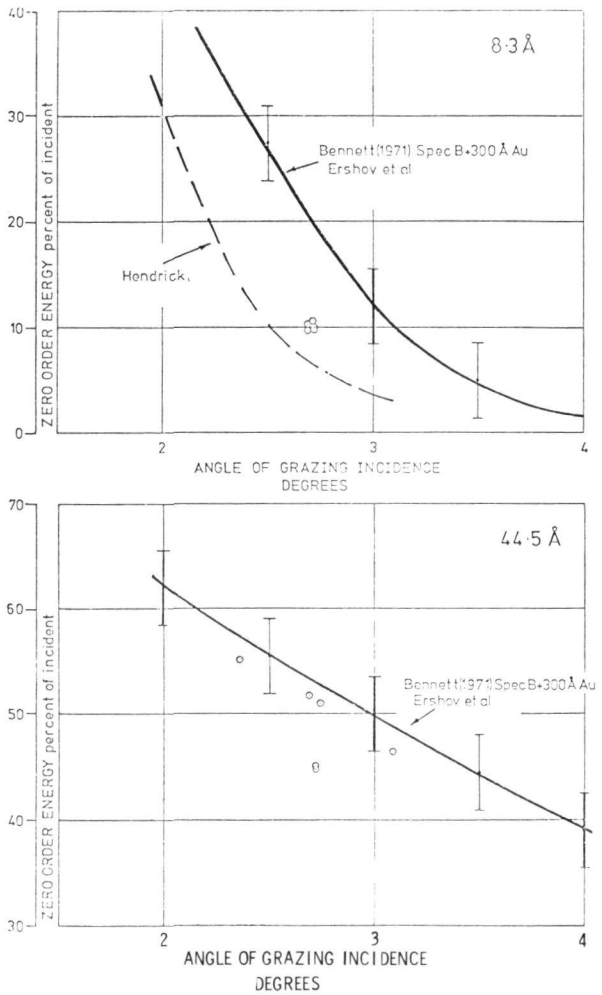

Figure 5. X-ray reflectivity measurements on XSST mirror (open circles) compared with other data.

Wavefront error in the mirror was examined in the grazing incidence interferometer at Imperial College. Using techniques discussed by R.J. Speer elsewhere in these proceedings, the XSST mirror was determined to be correctly figured to at least 0.7 micron of the desired paraboloidal shape at all points on its surface.

Acknowledgements

This research was supported by the National Aeronautics and Space Administration under Contract NAS2-9181 and the Lockheed Independent Research Program. The work of V.A. Stanley at Ion Tech, Ltd. in fabricating the mirror is gratefully acknowledged.

References

1. Giacconi, R. and Rossi, B., J. Geophys. Res. 65, 773 (1960).
2. Wolter, H., Ann. Phys. 10, 94 (1952).
3. Ershov, O.A., Brytov, I.A., Lukirskii, A.P., Optics and Spectroscopy, 22, p. 66, 1967.
4. Hendrick, J., Opt. Soc. Amer., 47, p. 165, 1957.